NTNU
Norwegian University of
Science and Technology

Mathematical Modelling of Cable and Pulley Systems.

Jon Andreas Moseid

I dedicate this work to my close friend Vidar, who encouraged me to start studying despite my turbulent relationship with the school bench.

Sammendrag

Innholdet i denne teksten møter utfordringen med todimensjonal FE-basert matematisk modellering av kabel og trinser. Teksten er hovedsakelig en forberedende studie for en kommende PhD-kandidat, hvor hoveddelen av fokus er isolert mot identifisering av teori basert på elementmetoden for å beskrive systemer som består av kabel og trinser. Arbeidet dreier seg om de iboende dynamikk- og friksjonseffekter som forekommer i slike systemer, og som forårsaker ute av fase svingninger i offshore tauverk. I løpet av studien har den mest hensiktsmessige matematiske formuleringen av modellering av kabel-trinse interaksjon blitt identifisert. Dermed er det et teoretisk grunnlag for den kommende forskningen ved SFI som dreier seg rundt dette og lignende temaer. Prinsipper for den foreslåtte modellen blir diskutert og forklart i detalj, med intensjonen for den følgende forskeren å enkelt overta arbeidet er utføret her.

Summary

The content of this text meets the challenge of two-dimensional FE-based mathematical modelling of cable and pulleys. The text is mainly a preparatory study for an upcoming PhD candidate, where the bulk of focus is isolated on identifying proper finite element theory for describing systems that consists of cable an pulleys. The work revolves around the inherent dynamics and friction effects between cable and pulleys, causing out of phase tension oscillations in an offshore crane. During the research, the most proper mathematical formulation of modelling cable-pulley interaction has been identified. Thus, provides a theoretical foundation for the upcoming research at SFI regarding cable-pulley systems. Principals of the proposed model are discussed and explained in detail, with the intent for the following researcher to easily adapt the work performed here.

Preface

This Master's thesis is a culmination of five years of study in the field of Mechanical Engineering, and was carried out during the spring of 2017.

The content originates from the request from the Centre of Research-Based Innovation (SFI), for accurate mathematical modelling of cable and pulleys. And also, the authors fascination of finite element modelling and simulation techniques during the studies. When introduced to the concept of digital twins, and its combination with the finite element method, it was considered an unique opportunity to get insight in an entirely new science domain.

The author would like to thank the supervisor, Professor Terje Rølvåg for the introduction to the topic, and for providing vital feedback on this work in order for this text to take shape. The author would also like to thank co-supervisor, Associate Professor Bjørn Haugen for the assistance regarding the mathematical challenge and extent of the work performed in this text.

Furthermore, he would like to address a special gratitude to his Canadian friend Meghan, who provided valuable help during the last days of writing. Also, this would not have been possible without his parents who has provided their everlasting support through the years of adolescence, and during the period of study. At last, a big thanks to cohabitants Thor Christian and Øyvind, who made the days of study cheerful.

Abstract

Within the last two decades, physical sensors has taken significant technological advances, becoming extremely accurate and at a low-cost thanks to the smartphone industry. Also, Internet and telecommunication are doing rapid technological advances. A result of these technological strides, several industrial revolutions has occurred, such as Industry 4.0, and the Internet of Things. However, due to the recent technological changing industry, the combination of smart algorithms, fast computers, accurate sensors, and an increasing reliability of Internet and telecommunication, enables for a new era of so-called digital twins.

The matter of modelling multibody systems assembled with cable and pulleys has for a long time been simplified, hence the focus on elements representing cable and pulleys has been in arrears. Thus, the Centre for Research-based Innovation (SFI) has addressed mathematical modelling of such systems as one of the most critical research and development tasks. An objective desired for the future is to accurately portray the inherent dynamics occurring, that significantly affects the behaviour of cable-pulley systems.

The work performed in this text documents state-of-the-art FE-based cable and pulley modelling. Further, it examines the effects that occur in a cable-pulley interaction such as inertial effects, cable dynamics, frictional impact etc. Based on the findings, a mathematical FE-based formulation of a two-dimensional model that may be used for further investigation of the topic is suggested.

By utilising ever-expanding computing power, this model can be implemented in software for helping engineers solve increasingly complex challenges related to cable and pulley systems. The model may also be implemented and applied in a script that includes a post-processor of sensor data instead of applying fictive loads, a digital twin. Thus, a long-term goal is to verify and optimise the FE-model for digital twin purposes, emulating real behaviour of physical systems in real-time. If this is achieved the long-term objective of this work is to obtain control synthesis for cable-pulley systems in the future. The model might be applied to control systems as a stabilisation algorithm for out of phase tensions and oscillations that occur.

Table of Contents

List of Figures

Abbreviations

ANCF	=	Absolute Nodal Coordinate Formulation
Black Box	=	A program that can be viewed in terms of its inputs and outputs, without any knowledge of its internal workings
CMS	=	Component Mode Synthesis
DOF	=	Degree of Freedom
FE	=	Finite Elements
FEA	=	Finite Element Analysis
FEDEM	=	Finite Element Dynamics of Elastic Mechanisms
FEM	=	Finite Element Method
GUI	=	Graphical User Interface
MBD	=	Multibody dynamics
MBS	=	Multibody systems
MDC	=	Minimal Distance Criterion
NURBS	=	Non-uniform rational B-spline
SFI	=	Center for Research-based Innovation

Chapter 1

Introduction

1.1 Background and motivation

Due to the rapid development of computer hardware and intelligent software has allowed scientists to conduct advanced calculations within the second half of the 20th century. The methods of multibody system dynamics have simultaneously been undergoing extensive development. This has resulted in a vast amount of different software tools specialised in the field of multibody dynamics, which is often applied in engineering during research and development. The finite element method is widely used within disciplines of engineering to perform advanced simulations, and to predict integrity of products and structures. The method is known to be computational expensive, particularly when detailed simulations include nonlinear effects i.e. plasticity in materials, nonlinear boundary conditions such as contact, and large motions due to complex dynamic systems. Thus, the focus on elements representing cable and pulleys has been in arrears, often simplified to be represented by few elements for the sake of computational time consume. This is an effective and agreeable approach in the construction industry, but does not emulate the actual behaviour of more complex dynamic systems. Thus, the Centre for Research-based Innovation (SFI) has identified mathematical modelling of the inherent dynamics in cable-pulley systems as one of the most critical research and development tasks. Numerous machines contain mechanisms composed of cables as driving elements, thus, it is necessary to obtain proper and effective modelling of cable and pulley systems for the interest of dynamic analyses, but also control synthesis. Control systems of such mechanical systems may be affected by various forms of undesired oscillations in elements such as flexible cables. Therefore, precise modelling of such systems is an applicable problem in nonlinear dynamics.

1.2   Limitations

The master thesis is independent from the specialisation project carried out during the fall semester and was therefore started from scratch in January. Thus, the original problem formulation was under uncertain conditions, and was targeted against digital twins. During the first period of the project, the bulk of focus was aimed on making a virtual crane modelled in FEDEM, interact with a physical crane through sensor instrumentation. However, during regular meetings with the supervisor, it became clear that creating a digital twin is not of interest, at such an early stage of the SFI project. The development of digital twins is undergoing extensive development within SAP Fedem, and is something that already has been done, hence do not contribute to innovation. Also, the physical crane was not finished in time, and documentation of FEDEM's communication with external software was inadequate for an external individual to apply these features. Therefore, it was agreed upon to isolate the focus on an FE-based element formulation of cable interaction with pulleys, that also is considered to be the most important task to investigate.

1.3   Problem formulation and objectives

The SFI Offshore Mechatronics project has identified mathematical modelling of cable and pulleys as the most critical research and development task. Cable and pulleys are critical elements when simulating offshore draw works and crane operations. The inherent dynamics and friction effects between cable and pulleys, may cause out of phase tension oscillations in the cables that cause control system instabilities. An objective is to identify a suitable formulation for describing such dynamics. Thus, this master thesis will contribute to the development of basic mathematical elements that are able to accurately portray these dynamics, deliberately computational efficient enough for a digital twin application. The main objectives of the research is following:

- Investigate and document state of the art FE-based formulation.

- Study and examine the inherent dynamic effects that occurs in a cable-pulley system.

- Present existing finite element formulations, and evaluate their pros and cons.

- Propose a FE-based mathematical formulation with adequate physical proximity, that are applicable for digital twins.

1.4   Report organisation and main contribution

The thesis is presented in the deliberate intent of a PhD candidate to work further with this topic. It is therefore assumed that the reader has significant scientific experience including mechanical and theoretical understanding. The first half of the text introduces the reader to the scope of the assignment, i.e. state of the art modelling, examination of physical effects that occurs in a cable-pulley system. It then presents a model that is, in the author's opinion, the most suitable formulations for simulating such systems. To get a fundamental understanding of the model proposed in this thesis, it is recommended for the reader to

have previous knowledge and experience of linear algebra and the finite element method before reading this text. The content of this text is structured as follows:

Chapter 2, presents the author's philosophy and approach for dealing with the problem formulation, and discusses some of the methodologies applied for achieving the objectives.

Chapter 3 discusses the concepts of a digital twin, presents its potential for future industry, and current limitations regarding the issues of cable and pulley simulations.

Chapter 4, explores the previous work performed by other researchers related to this problem. This chapter documents state-of-the-art on cable pulley modelling and simulation, and provides the reader an overview of different possible approaches which may be further applied for this purpose.

Chapter 5, covers the dynamic effects occurring in a cable-pulley system that needs to be taken into account, and introduces the reader to the theoretical framework for the further development of a finite element based model.

Chapter 6, consider some of the elements that have been investigated during the research, the elements ability to cope with the physical effects presented are compared, and a conclusion is obtained.

Chapter 7, provides a full presentation of the chosen element identified to be most suitable for the model. It also covers how to model a pulley compliant with the element formulation.

Chapter 8, covers how to describe contact kinematics, contact forces such as normal- and frictional forces, and at last, the kinematic constraints between a cable and pulley are defined.

Chapter 9, discusses simulation techniques, how they are performed and the introduction of stabilisation techniques. It also discusses algorithms suitable for real time simulations.

Chapter 10, brings back the content of the text, discusses the discoveries and lessons learned during research, with the intent for further work.

Happy reading

Chapter 2

Research Methodology

In the kingdom of the blind, the one-eyed man is king.

— *Desiderius Erasmus Roterodamus*
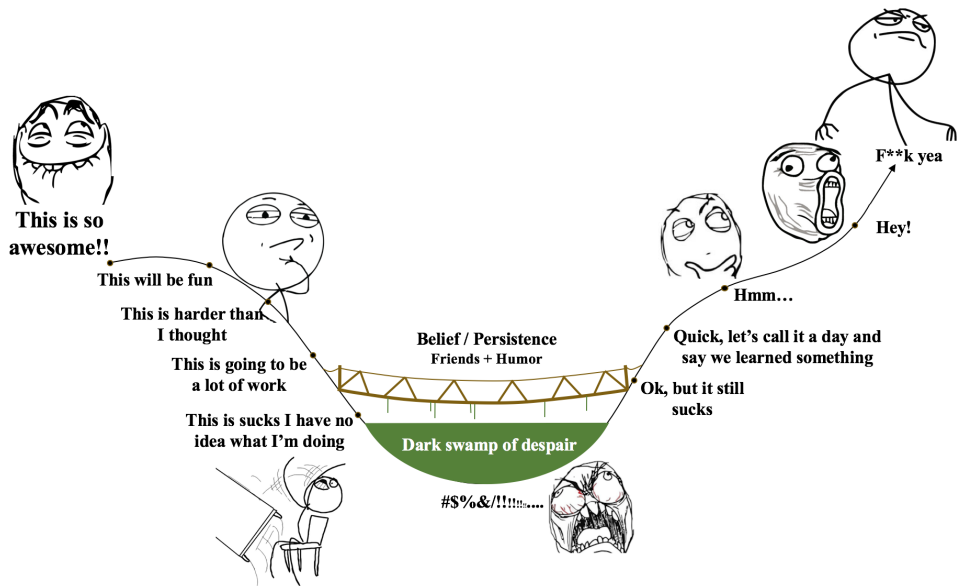
Figure 2.1: The inevitable emotional journey of creating anything great.

2.1 Identification

As discussed in Chapter 1, a challenge has been addressed, however, its extent has to be identified in order to frame the problem and further establish the scope of research. This will be discussed in Chapter 3 in order to validate the need for this research and development. Further, in order to deal with the challenge, scientific methods must accommodate the basis for research, and knowledge for development. The aspects of the methods that are applied is will need to be addressed in order to ensure the credibility and verify the author's procedure. In any sort of development, verification and validation of the project requires evaluation, Kerzner [1] summarized these terms in the following way:

- **Validation**: *"Are you building the right thing?"*

- **Verification**: *"Are you building the thing right?"*

2.2 Exploration and theoretical framework

Within the field of engineering, March and Smith [2] argues that the associated research methodology is to examine already existing developments and artefacts, rather than studying the natural world. However, in order to improve current systems, a proper understanding of the natural world is essential for obtaining achievements. Eisenhardt [3] states that the development of theories based on observations in other literature, common sense, and experience is a traditional methodology. She also emphasises that validation afterwards the developed theories against experimental results, establishes a good quality of research. In order to express the inherent dynamics of a cable-pulley system mathematically, knowledge is the backbone, such as any challenge in engineering. An exploration process should start with a broad focus, yet focus in on the specific problem. In this work, the exploration methodology is simply to investigate previous works, explore strengths and weaknesses of other state-of-the-art models, and study its demand of further development, in order for improving their potential and integrity.

2.3 Development

In any concept development, first one analyses the challenge and all aspects around it, secondly, one analyses possible solutions to the challenge, referred to as concept exploration. Furthermore, the solutions are carefully considered against the challenges in order to identify the most suitable solution method. Three stages consisting of three subordinate phases is illustrated in figure 2.2 and provides a graphical overview a development process, adopted from the field of Systems Engineering [4].

The Need Analysis Phase examines if there is a valid need for new development, and investigates if there are any practical approaches that satisfies the need (Chapter 3).

The Concept Exploration Phase examines potential approaches that exist and is able to cope with the challenge (Chapter 4). It also studies the required performance for a new development to meet the perceived need (Chapter 5). It then investigates if there is at least one feasible approach that satisfies the performance (Chapter 6). The output of this phase
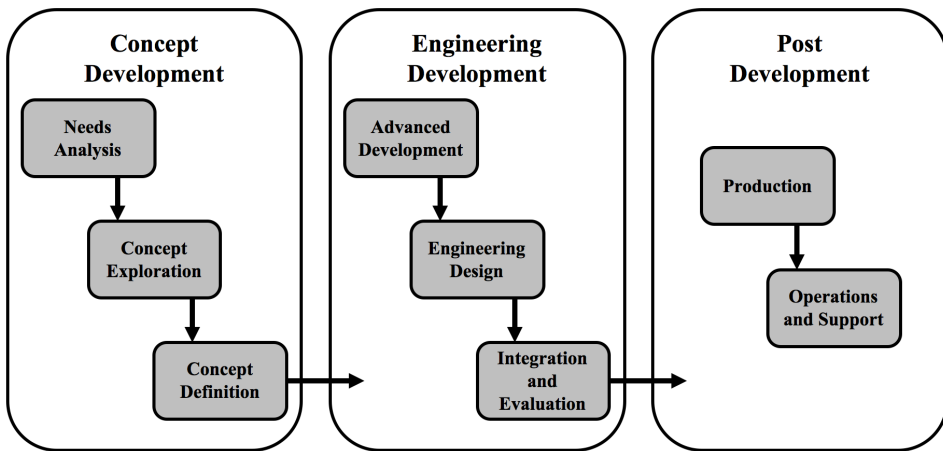
Figure 2.2: System life cycle model [4]

provides a first "official" set of requirements, commonly known as performance requirements.

The Concept Definition Phase selects the preferred approach for solving the problem, based on the key characteristics of a concept that would achieve most beneficial balance between capability, operational life, and cost (Chapter 6).

Kossiakoff [4] summarized the principal objectives of the concept development stage as follows:

- *to establish that there is a valid need for a new system that is technically and economically feasible;*

- *to explore potential system concepts and formulate and validate a set of system performance requirements;*

- *to select the most attractive system concept, define its functional characteristics, and develop a detailed plan for the subsequent stages of engineering, production, and operational deployment of the system;*

- *to develop any new technology called for by the selected system concept and to validate its capability to meet requirements.*

This work is considered, thus treated to be at the stage of concept development. Thus will adopt and execute the presented methodologies in order to identify a mathematical simulation technique suitable for covering an "official" set of requirements.
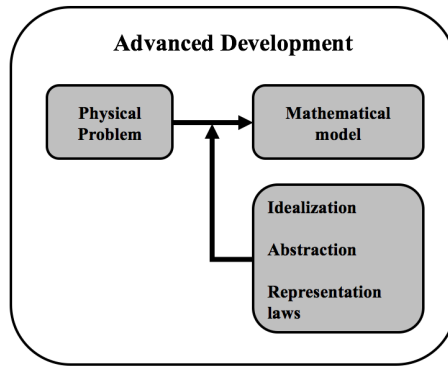
Figure 2.3: Concepts involved in the construction of a mathematical model [5]

The Advanced Development Phase (Chapter 7, 8, 9) is critically dependent on the foundation established in the stage of Concept Development. However, the conceptual effort is of a broad analytic nature and often carried out with limited resources. Thus, significant unknowns remain to be fully defined and resolved, it is therefore essential that these "unknown unknowns" are exposed at an early stage.

2.4 Discussion and conclusion

During discussion, the content and context of the research should be brought back again [6]. It exposes the lessons learned, and through discussion, they should be put in a broader perspective. Thus, the discussion enables for new researches and further work. The conclusion brings back the context by reviewing the development objectives and evaluates the satisfaction of these. In engineering, a conclusion is often associated with physical testing and comparison in order to verify a new development.

Chapter 3

The concept of a digital twin

*Digital twins are becoming a business
imperative, covering the entire
life-cycle of an asset or process and
forming the foundation for connected
products and services. Companies that
fail to respond will be left behind.*

*— Thomas Kaiser, SAP Senior Vice
President of IoT*

A digital twin is simply a bridge between the physical and digital world. The idea is to
utilise data from sensors and actuators installed on a physical object to represent their
near real-time status, working condition, and position of a product, process or service.
A physical object has to be instrumented with sensors that gather real-time data, the re-
ceived monitored data is transmitted to a software or a cloud-based service that processes
the input, and analyses it against other contextual data. The future vision of digital twin
is diverse and applicable in a large range of different disciplines and industries, and is a
relatively new idea which has barley been exploited up to this point of time. SAP Fedem
applies the monitoring approach which aims at providing an integrated overview of the
structural integrity of a construction or mechanism at any time. The software that analyzes
the processed sensor data is known as FEDEM, based on the finite element method, which
enables the use of so-called *virtual sensors*, decreasing the need of an unnecessarily large
amount of physical sensors. It also applies model reduction that reduces the system of
equations to a minimum, making it remarkably suitable for real-time simulations of dig-
ital twins. However, there are some challenges from time to time when a digital model
demand element formulations that exceeds the characteristics of embedded elements, in
order to adequately represent a physical model. In this chapter, a digital twin prepared for
actuation is presented, however, the underlying theory of sensor technology, data filtering,
and actuation will not be presented.

3.1 FEDEM

FEDEM is the acronym for Finite Element Dynamics of Elastic Mechanisms and is traditionally a simulation tool for more complex mechanical assemblies. FEDEM consists of a rather intuitive GUI, illustrated in figure 3.1. The software can be categorised as a Multi Discipline Simulation tool, combining Multibody Simulation (MBS) which has traditionally treated an assembly consisting of rigid bodies, the Finite Element Methods (FEM) that accounts for deflection in components, and Control Engineering. Simulations in conventional FE-software is normally time-consuming procedures, due to large sets of differential equations that needs to be solved. However, FEDEM is applying a methodology for eliminating the simulation time drastically due to an algorithm that reduces the system of equations through CMS model reduction.
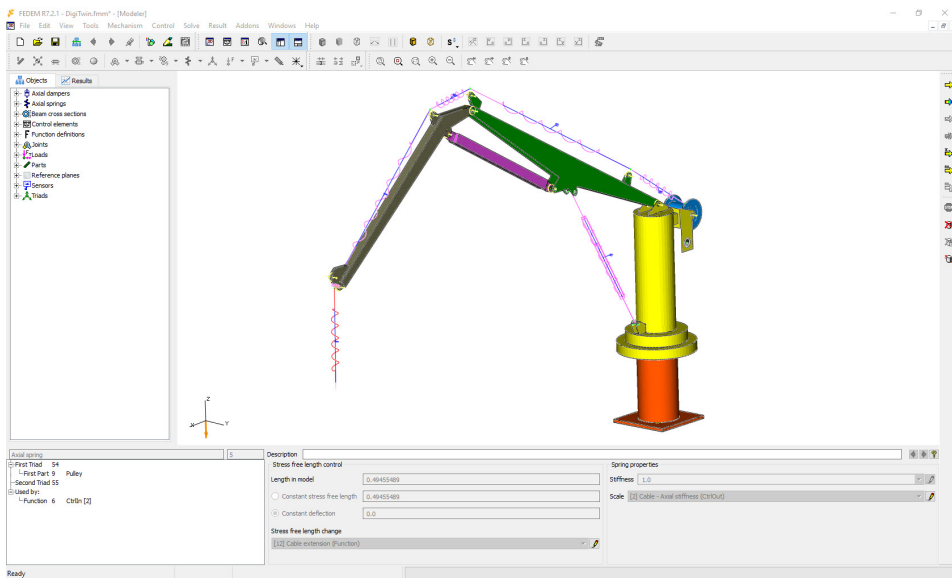
Figure 3.1: Graphical user interface of FEDEM

3.1.1 Model Reduction

A simulation model based on finite elements in a conventional simulation software, do have a large amount of differential equations that needs to be solved for every time step in a dynamic simulation. Every node in a FE model contains a set of up to six DOFs, dependent on the chosen elements for the model. A FE-modelled system may contain several thousand DOFs, making the system of equations extensively large. FEDEM introduces a Component Mode Synthesis (CMS) model reduction in order to cope with this issue [7, 8]. In order to decrease the equation, the nodes are categorised as internal and external nodes, and divided into sub-matrices. The external nodes, also referred to as *supernodes* or *triads* are defined as external DOFs when an interaction is manually assigned to the body, further

the physical properties of the external nodes are defined through the internal DOFs. The internal DOFs are eliminated from the system and replaced by a limited amount of the lowest vibration modes of the substructure. The fundamental assumption is that the lowest natural frequencies are the important ones, also the higher frequency modes are less accurate in numerical models [7]. The full derivation of the CMS transformation can be found in several literature's, e.g. Sivertsen (2001) [8]. The model reduction results in a total elastic behaviour of the components. However, normally in the field of mechanical engineering, if a component exceeds the yields stress and ends up in the plasticity region of the material, it is usually not designed properly, making this simplification reasonable. The overall behaviour of the assembly is considered highly nonlinear due to the large motions of the dynamic models simulated.

3.2   Finite element model of the crane
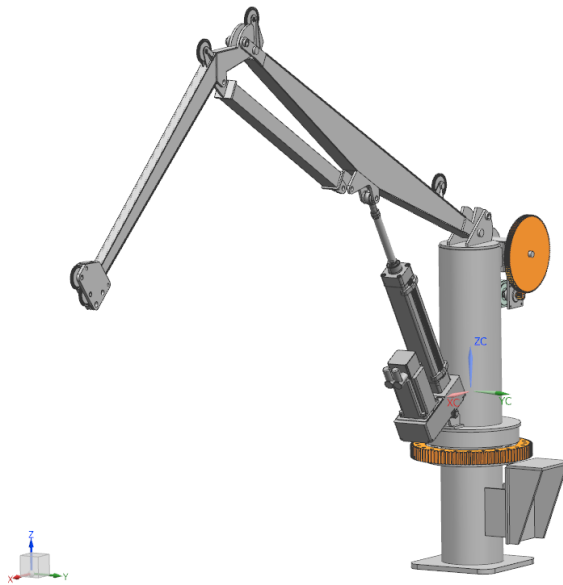
Figure 3.2: CAD model of a scaled lab crane.

A detailed CAD model of a scaled crane was provided by PhD candidate Andrej Cibicic, the model was mainly intended for production and had to be idealised for meshing. The idealisation process was performed carefully in order to maintain the structural integrity of the model. The idealisation and meshing process were performed with Siemens NX, before it was exported as Nastran files for FEDEM to read. Figure 3.3 illustrates the final model of a digital twin in FEDEM.
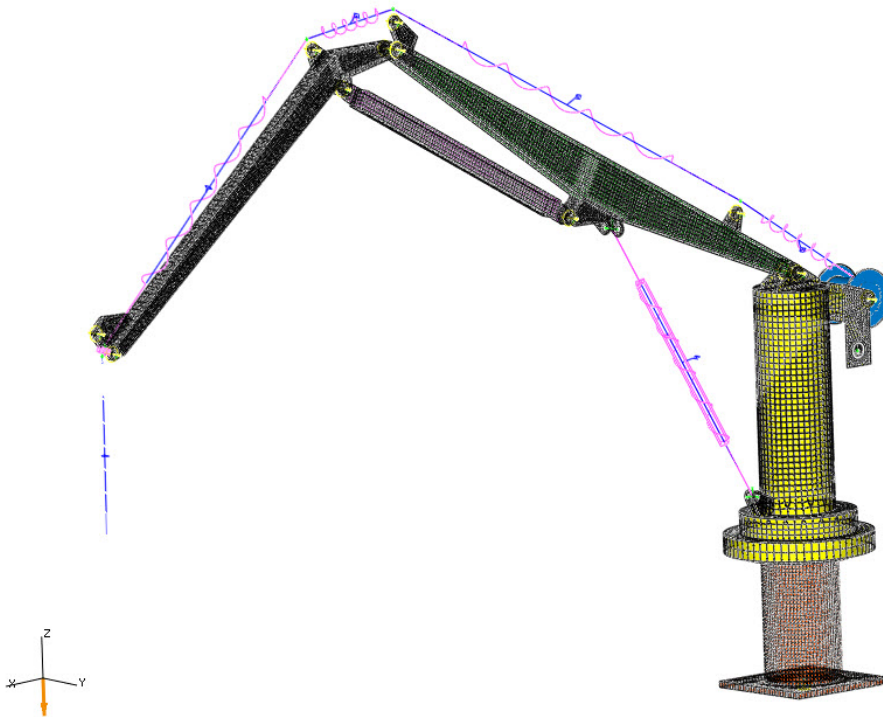
Figure 3.3: Assembly FE-model in Fedem.

3.2.1 Element selection

For an accurate digital twin, it is essential to obtain a certain accuracy, simultaneously as it is computationally efficient. FEDEM does not support certain elements that are common in conventional FE-software, which is necessary to have in mind when meshing the parts in a third party FE-program. The parts have mainly been meshed with 4-node C^0 quadrilateral elements in Siemens NX, before it was exported over to FEDEM. The properties of these elements have some limitations, i.e. it is confined to describe mechanical behaviour in its own defined plane, but provides adequate structural integrity if the element size is chosen with care. For instance, the element size illustrated in figure 3.3 is believed to be of too fine fore a digital twin, and needs to be coarsened. However, these elements are advantageous in applications for digital twin purposes, due to its decreased amount of DOFs, which advances the computational efficiency when solving for stresses and strains in the post-processors.

3.2.2 Control system

FEDEM has a built-in control system which closely resembles basic control theory, and is similar to Simulink. The control system provides very powerful tools for the simulation of multibody systems, making it very handy for a user during the setup of a simulation.

Its graphical representation consists of control blocks of different functions, connected in series for obtaining the desired simulation of the behaviour of a system.

3.3 Actuation of a digital twin

(a) Real system   **(b)** Digital twin
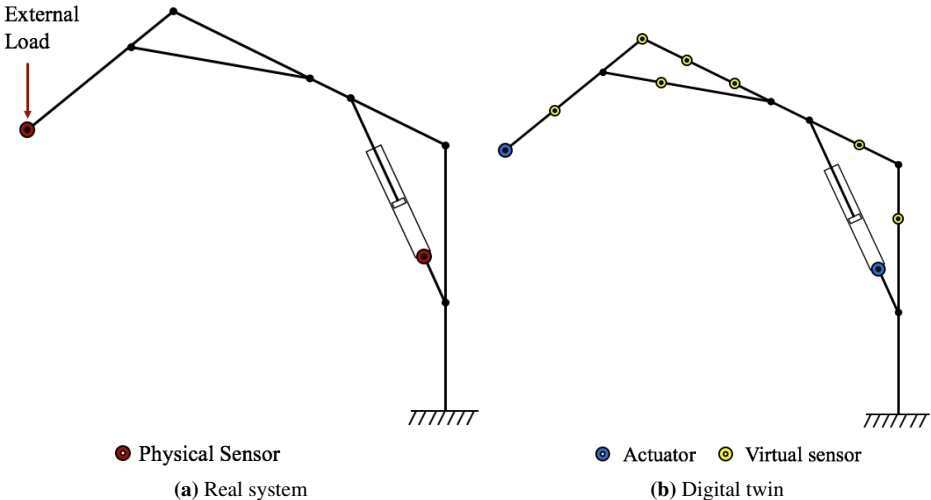
Figure 3.4: Illustration of the

The digital twin illustrated in figure 3.4b is represented as a numerical model with the exact physical dimensions, material data, constraint conditions etc. to mimic a physical system illustrated by figure 3.4a. In order to actuate the digital twin, instead of fictitious load conditions, one applies physical sensor data that monitors the dynamic responses, material deformations, state conditions etc. of the physical system. However, the sensors can also be of a virtual kind that is placed in arbitrary positions of interests on the digital twin. Thus, by combining numerical models with physical sensors, one can observe real-time mechanical conditions of an entire structure or machinery during operation. If one succeeds with the challenge of modelling an accurately adequate cable-pulley system, one can further combine the model with sensors and actuators for obtaining digital twins of such systems.

3.4 Modelling cables and wire ropes as linear springs

A commonly known property to structural elements such as cables is their ability to withstand large axial loads in comparison to bending, compression, and torsional loads. A well-known approach for modelling cables is by simplifying them into linear or bi-linear springs [9, 10, 11], considering the stiffness to be dependent on the length and neglecting

the mass and inertial forces. Hence, the approach results in very efficient simulations, and its accuracy is adequate for common engineering applications [12].
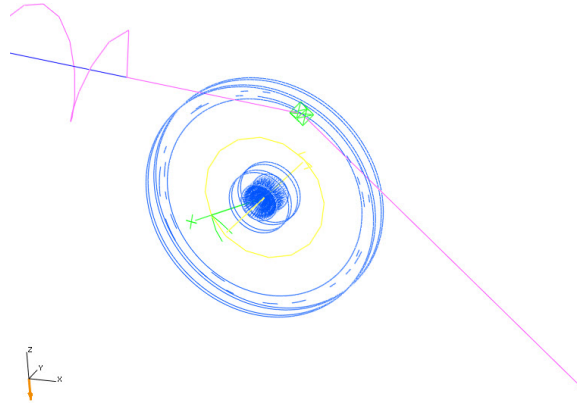
Figure 3.5: Cable-pulley interaction in FEDEM

Figure 3.5 illustrates how the cable pulley interaction has been modelled in FEDEM. The cable is modelled as bi-linear springs, the stiffness depends on its extension, and is connected to a *triad* on a pulley with a rotational degree of freedom. The pulley is attached to its supporting structure i.e. the crane, through a revolute joint. This is a rather simplified approach and does not represent a real system. However, it can provide indications of some dynamic effects occurring (Section 5.5.4), and was therefore used instead of attaching the cable directly to the pulley fixing point on the crane. As mentioned, the simplification of the cables neglects bending stiffness, thus does not consider the lateral vibrations of the cable, the friction acting between the cable and pulley is neither included in this simplifications. If a system for modelling drawworks, belt-drives, elevators, cable-driven robots and control systems for autonomous vehicles, just to mention a few, this method is inadequate. Therefore, SFI has addressed the importance of research and development of FE-based mathematical models to cope with these challenges.

Chapter 4

Literature Review - Previous Work

> If I have seen further, it is by standing on the shoulders of giants.
>
> *— Sir Isaac Newton*

This chapter provides a rapid review of state-of-the-art cable pulley modelling of modern times. The literature reviewed will not be discussed in detail, and is intended for the reader to get an overview of some of the existing approaches and methods. Thus, if some of the literature is of special interest, it is intended for the reader to go directly to the source for details. Some of the most conventional elements used for modelling cable and pulleys will be revealed, although the discussion of potential elements will be carried out in Chapter 6.

4.1 Ju and Choo (2004 / 2005)

Ju and Choo [13] developed a super element approach for describing the overall impact of a large multiple-pulley cable system on its supporting structure. The authors addressed other approaches which modelled the cables as linear springs, fixed beams, or modelling multiple-pulley cable system by neglecting friction when passing through pulleys as inadequate methods which provided inaccurate results. This was handled by imposing frictional relations between the cable tensions at the two sides of the pulleys. However, a year after, the same authors performed a dynamic analysis of a tower crane [14] by applying the super element approach, yet neglecting the frictional loss over the pulley without any argumentation for the simplification. Dynamic responses and modal properties of the crane were examined, and cases of sudden accelerations of the payload were studied. However, it is stated in their articles that the chosen methods used for modelling cable-pulley passages, has significant effects on the behaviour of a structure as a whole.

4.2 Kerkkänen et al. (2006)

Kerkkänen et al. [15] developed a model for simulating belt-drives. The author addressed the lack of realistic models for describing such systems, and its requirement for exact modelling by including sheaves to the system, ability to describe nonlinear deformations and realistic contact. The tensions of a belt during operation is going through transitions from large to small tension and *vice versa*. Thus, the belt is subjected to fatigue and the tensions of the belt-drive are critical for determining its lifetime, another factor is the creep between the belt and pulley causing sliding wear. The need for a sophisticated method of surveying all the forces appearing in such systems was needed for predicting all aspects of the long-term design integrity. An ANCF element capable of modelling highly nonlinear deformations, proposed by Dufva et al. [16], were applied for modelling the belt. The element was chosen due to its high-order (C^2) formulation, enabling for accurate contact description, yet with a low amount of elements required. However, since the pulley is considered as the systems driving element, only its geometry and angular velocity were taken into account. By this approach, all the above mentioned requirements were obtained, providing adequate numerical results for the modelling and simulations of belt drives.

4.3 Imanishi et al. (2009)

Imanishi et al. [17] developed a dynamic simulation model for wire ropes subjected to rapid winch accelerations. The cable was modelled as a variable-length truss element i.e. similar to a bi-linear spring, revolved around a winch drum. Its configuration was described through nodes representing pulleys mounted on a crane structure. The contact between the winch drum and the cable were modelled by additional variable-length truss elements, connected between the winch drum centre point, and the nodes of the cable. These contact elements were programmed to contain zero stiffness unless their length occurred below a prescribed radius of the drum. And if so, the element would become excessively stiff in the direction of compression, and the cable were obtained in a con-

strained position around the drum. Yet, there was zero stiffness in the direction of tension, which allowed the cable to "jump off" if the winch drum was subjected to sudden surges and accelerations, enabling for nonlinear analysis of the tensions in the cable, yet unable to describe friction. The motion of the winch drum was described by a mathematical model of a hydraulic system, and dynamic simulations were performed in order to examine the rope looseness occurring during rapid winch operations.

4.4   Sun et al. (2011)

Sun et al. [18] formulated a nodal position finite element (NPFEM) motivated by the need of an alternative robust formulation as means to analyse the dynamic behaviour of cables experiencing large rigid body rotation, combined with small elastic deformations over a long time of period. This formulation calculates the position of a cable directly instead of its displacements as conventional beam elements. The element properties were chosen to absorb elastic strain, but only in the longitudinal direction. The element was implemented in a simulation program with moving boundary conditions, representing a submerged rigid body and its associated dynamics, towed by a moving vessel. Simulating the nonlinear dynamics in the cable of the towed body system were preformed and compared with physical trials. The element proved to be accurate and robust in comparison with experimental results.

4.5   Lugrís et al. (2011)

Lugris et al. [12] addressed in their article the need of an improved model of cable and pulleys due to the energetically inconsistency, generating spurious terms in the system equations of existing simulation methods, that applies linear or bi-linear springs for the modelling of cables. At first, an elevator system modelled with wire ropes simplified to bi-linear springs, motion dependent on the angular velocity of the motor, driving the system. This model demonstrated the inconsistency of energy conservation. Subsequently, a numerical model based on the ANCF proposed by Shabana [19], were developed. In contrast to Kerkkänen et al, the pulley were considered as a driving element, but included inertia. The ANCF were chosen due to its capability of capturing detailed interaction with a pulley and its nonlinear behaviour. The developed cable-pulley system proved conformance in the energy balance.

4.6   Wang et al. (2014 -)

Wang, Tian, and Hu [20] proposed in 2014 a method for describing frictional contact between two spatial thin beams with a circular cross-section, that is subjected to large deformations, i.e. spatial models of ropes interfering with each other. Their method was based on contact detection between ANCF beams by applying the minimal distance criterion, then applying a master-slave approach, that determines which one of the beams to dominate the contact. Furthermore, the penalty method was used for defining the normal

and frictional contact forces between the objects. Their research concluded that by applying this element proved to be promising and was followed up by an improved formulation including multi-zone friction in 2016 [21, 22].

4.7   Arena et al. (2015)

An investigation carried out by Arena et al. [11] looks at improving the efficiency of container cranes for handling cargo. The research team addressed the need for optimisation due to inherent dynamic behaviour caused by the structure and its hoisting system, influencing the productivity of an overall terminal. Their approach included a full-scale, three-dimensional container crane. The hoisting cables were both modelled as straight taut cables or straight rigid rods for comparison. Physical tests were performed for several crane configurations in order to determine parameters for the system, and experiments were carried out for obtaining sensor data, and in order to verify the model. The proposed model enabled parameterisation of the dynamic responses of the heave for different manoeuvres and wind disturbances.

4.8   Myhre (2016)

Dr. Myhre [23] performed recently a research at NTNU regarding robots interacting with humans. The purpose of his study was to investigate how a human can interact with a robot for increasing efficiency in industries by sharing the load, specifically handling long and slender beams in stacking operations. The goal was to let a human lead the robot through a trajectory by motion. By obtaining this goal, the motion of the flexible beams were tracked by the help of artificial vision, while the beams were formulated by applying the ANCF for compute its spatial position and deflection, making the motion tracking more robust. The experiments were successfully performed by this approach, and proves its efficiency and performance for applying to real-time simulations.

4.9   Bulín et al. (2016 -)

Bulín et al. [24] acknowledges in their paper that the ANCF is an effective element for simulating systems consisting of cable and pulleys. However, the authors address the lack of experimental comparisons in order to fully validate the method. Their approach was to develop an in-house simulation tool, and the cable they used was modelled as a flexible ANCF-based beam. To describe its interaction with a pulley, the normal and friction forces were obtained by defining contact forces based on the Hertz theory of contact. In contrast to Lugrís- and Kerkkänen et al. the considered driving element was modelled external motor imposing movement on the cable. Thus, the pulley movement were purely caused by the cable interaction. A mechanical system composed of a driven weight and joined with a motor, led over a pulley was then investigated and compared. The results combined with the numerical model shows sufficient agreement and demonstrated a good capability of simulating the highly nonlinear behaviour of a cable. This investigation proved that the ANCF model is suitable for dynamic analyses and simulations of such systems.

Chapter 5

Physical analysis and theoretical framework

Research is creating new knowledge

— Neil Armstrong

Work performed by other authors have been presented, and a full understanding of the characteristics of a cable-pulley system needs to be examined. An understanding of the effects is crucial before moving on to more complex mathematical formulations of the problem. This chapter gives an introduction of the various dynamics that have been considered for this project.

5.1 Fishbone diagram
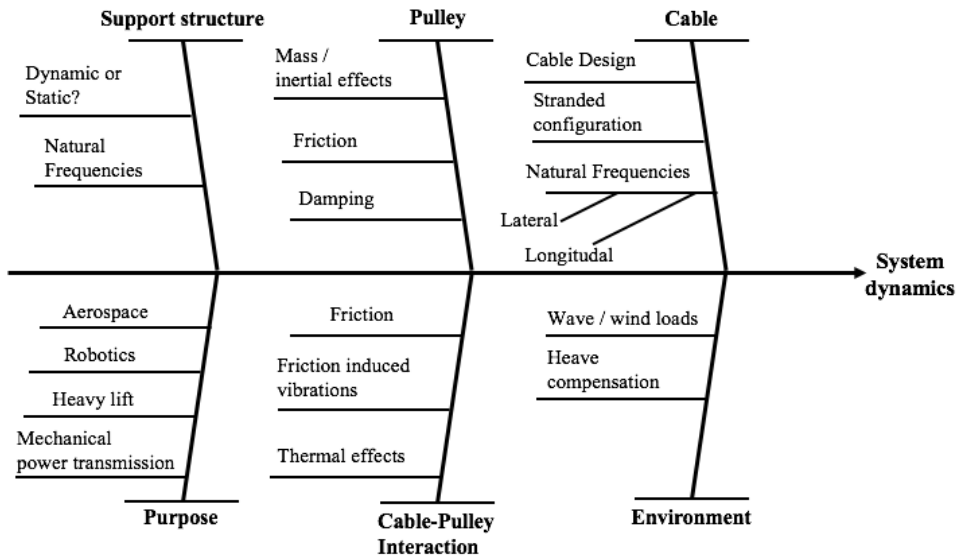
Figure 5.1: Fishbone diagram for effect survey.

A fishbone diagram used to facilitate root cause analysis of system dynamics is illustrated in figure 5.1. This is a helpful tool for analysing any challenges regardless the level of complexity. The overall system dynamics is a product of many different effects that has a variety of impacts on the overall system. One has to determine which of these effects is the most critical for the overall behaviour, then investigate them in order to establish the building blocks for the development and mathematical modelling. The bulk of focus should be to examine and understand the more dominating effects in the system to obtain a mathematical foundation which can be customised for its purpose. It is therefore required to better understand the individual phenomenons, some of them occurring at a micro mechanical level, in order to better understand the behaviour of a full-scale system. Thus, the focus will isolate on the inherent effects that are independent from external influence.

5.2 Cable Dynamics

Systems involving components such as ropes and cables often exhibits unwanted frequency vibrations, due to its mass stiffness proportional relation that needs to be considered. In many cases involving cable and pulleys with large lifting ranges, will most likely pass through a resonant vibration stage at some point of its travel. Whatever the subordinate cause of the vibrations, it will normally excite the associated oscillations of the cable structure [25]. The heave may also have some slight pendulous movements that cause fluctuating cable tensions. Considering that the oscillations are independent from

the configuration and direction of the cable, at any stage of the systema, yields the natural frequencies and its mode shapes.
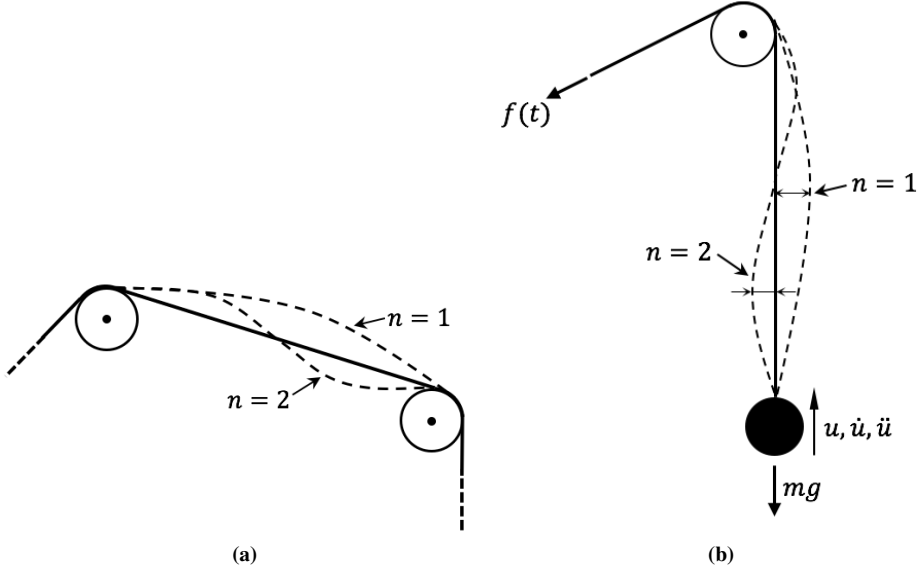
Figure 5.2: Illustration of lateral oscillation, mode 1 and 2.

From *Newtons second law*, the sum of all the forces acting in a system yields

$$m\ddot{u} + c\dot{u} + ku = f(t) \tag{5.1}$$

where m, c and k is the total suspended mass-, damping- and stiffness of the cable, respectively. u, $\dot{u}$ and $\ddot{u}$ is the displacement from any reference position of the load, velocity, and acceleration respectively, with respect to time. Using this equation, one can calculate the natural frequencies (see Section 5.6) by neglecting the damping of the system in equation 5.1, putting the external loads to zero. Thus, the basic expression for the natural frequency in its longitudinal direction of the cable yields

$$\omega_{axial} = \sqrt{\frac{k}{m}} \text{ rad/s} \tag{5.2}$$

in addition, one can expect lateral oscillations will occur on the cable [25], expressed in an analytic form

$$\omega_{lateral} = \frac{n\pi}{L}\sqrt{\frac{\text{Cable Tension}}{\text{Cable Mass}}} = \frac{n\pi}{L}\sqrt{\frac{Mg_n}{n_c m_c}} \text{ rad/s}, \qquad n = 1, 2, 3.... \tag{5.3}$$

where n denotes the different modes and L is the length of the cable. In the case of multiple suspension cables i.e. if the system contains multiple sheaves mounted in parallel

e.g. a crane block, n_c denotes the quantity of parallel cables, and ρ_c is the cable density. Considering a cable pulley system with large travels of the heave, the length and mass of the cable is considered as variables with respect to time, $L(t)$ and $M(t)$ respectively. Thus, the mean tension of a cable is expressed

$$T_{mean} = M(t)g_n + \frac{L(t)}{2}n_{sr}m_{sr}g_n \tag{5.4}$$

substituting into 5.3 yields

$$\bar{\omega}_{lateral} = \frac{n\pi}{L(t)}\sqrt{\frac{M(t)g_n}{n_c m_c} + \frac{L(t)g_n}{2}} \text{ rad/s}, \qquad n = 1, 2, 3.... \tag{5.5}$$

It is worth noting that when oscillations occur in a cable, it becomes dynamically deformed. During deformation, it stores potential energy due to its elastic properties. Worst case scenario, the elastic behaviour of a cable may contribute to amplifying its own oscillation amplitudes if a resonant vibration stage is kept stationary in a period of time, whatever the underlying reason.

5.3   Cable configuration and bending stiffness

The main purpose of a cable is the transfer of forces in its axial direction, thus the cables are taut in general. It is common sense arguing that cables are unable to withstand bending and compression. For instance, Gerstmayr and Shabana [26], argue that the effect of bending stiffness can be neglected in high tension cable problems, but the effect of bending stiffness becomes more important in cases of low tension. However, this is only true in a global sense, and the effects of bending can arise in some or several segments of the length of a cable. As noted, some authors [9, 14, 10, 11] neglect the bending stiffness of an element, while others [20, 15, 24, 12] have incorporated stiffness and damping properties based on estimates and approximations to their models. This helps tune the properties and emulate cable dynamics. When neglecting bending stiffness in an element, its rotational degrees of freedom in the nodes disappear, and the lateral behaviour of a cable is eliminated from the system equations.
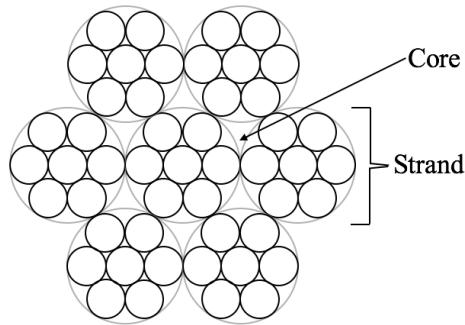
Figure 5.3: Anatomy of a cable [27].

(a) Inter-layer friction zone.

(b) Cross section of a strand.

(c) Helix shape [28].
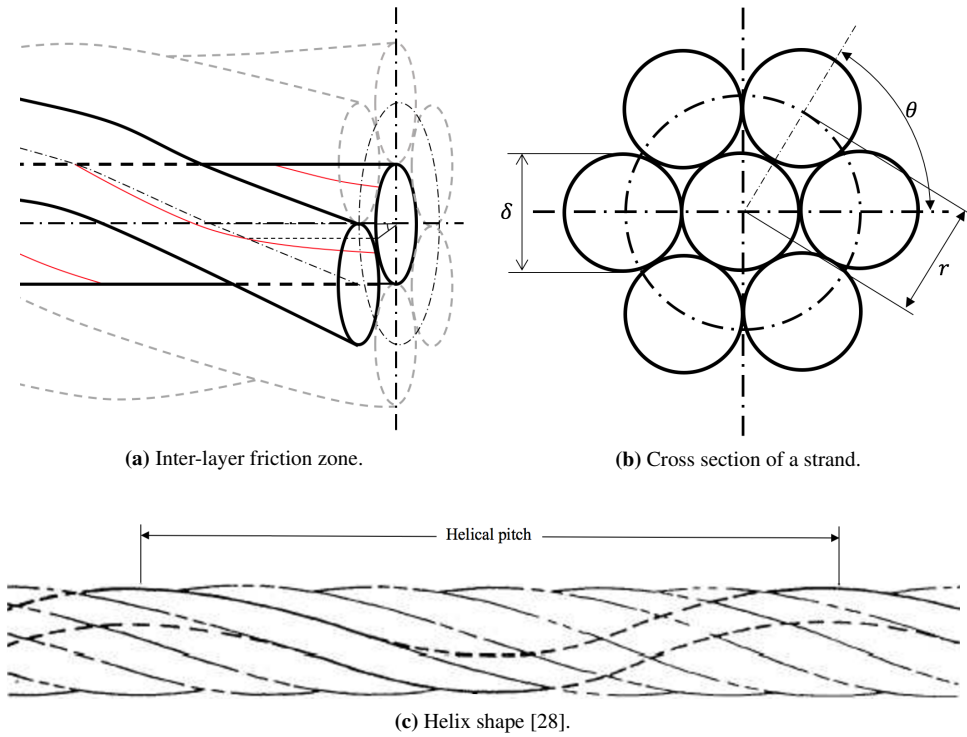
Figure 5.4: A single-helical rope configuration.

For describing configurations of a cable, the designation is $m \times n$, where m denotes the number of strands, and n the number of wires in each strand. The cross section illustrated in figure 5.3, shows a 7×7 stranded cable [27].

A cable may have various configurations, different coating, as well as wire rope of naked steel. In offshore applications these cables often contain grease in the core and inter-layers of wires for increased corrosion resistance and a smoother behaviour. In any conventional FE- formulation, the elements are derived as homogeneous cylindrical bar or beams, which is not the case for a cable that is neither isotropic, nor homogeneous. As means to accurately portray the dynamic responses in a cable, the mechanical parameters which are incorporated in beam formulations have to be modified for this purpose. A well known expression for bending in beam elements, and a well known approximation for the modelling of cables [29] has the form

$$M = EI\kappa \tag{5.6}$$

Where M denotes the bending moment, EI the bending stiffness and κ the curvature of the beam. The beam model provides useful dynamic response data which incorporates tension, internal damping, and connection points [27]. However, applying conventional equations for calculating the stiffness based on a circular cross section provides unrealistic stiffness to a cable. This has been addressed in other articles [12, 24] working with cables,

scaling down the bending stiffness drastically to obtain more realistic behaviour. Thus, scaling the second moment of area I by a factor of 25 by approximation for obtaining more realistic beam characteristics, proves adequate conformance with experimental results provided by Bulín et al. However, in when bending increases in a cable, the internal friction acting between the wires is not equivalent for preventing a relative slip between the wires and the cores. Relative slip occurs when a wire crosses the neutral axis of a cables cross section [29]. Papailiou [29] was the first to propose an analytic model for conductors accounting for the inter-layer stick-slip friction, resulting in a variable bending stiffness. The model was implemented as a planar beam in a simple FE-code as a nonlinear quasi-static analysis, proving promising conformance with quasi-static experimental tests. His research proved that bending stiffness is altered when subjected to bending displacement and tension. Spak et al. [27] proposed a method for determining the effective homogeneous beam parameters for the purpose of modelling a stranded cable, and pointed out that damping properties caused by friction and viscoelastic shear effect should be incorporated when modelling wire ropes. The parameters were used in beam models for predicting natural frequencies of cables mounted in space crafts, studying its influence on the entire structure. Foti et al. [30] recently proposed a new refined model describing the mechanical behaviour metallic stranded cables subjected to tension, torsion, and bending. The model fully accounts for the composite nature of multi-stranded wire ropes, subjected to hysteresis bending behaviour. By summarising the stiffness contribution from each wire yields an overall bending stiffness of a cable. The relationship between minimum stiffness properties and the geometrical configuration, contributed by the sum of slip friction between the inter-layer wires in a cable subjected to bending, yields

$$ EI_{min} = \sum_{j=0}^{m} \frac{n_j}{2} \cos \alpha_j EI_{w,j} \left[1 + \cos \alpha^2 + \frac{\sin \alpha}{1 + \nu_j} \right] \tag{5.7} $$

and the maximum bending stiffness contributed by the sum of stick- and slip friction between the inter-layer wires.

$$ EI_{max} = EI_{min} + \sum_{j=1}^{m} \frac{n_j}{2} \cos \alpha_j{}^3 EA_{w,j} r_j^2 \tag{5.8} $$

With the following input parameters (see figure 5.4)

$$
\begin{cases}
n_j & \text{number of wires in the } j^{th} \text{ layer} \\
\alpha_j = \tan^{-1}\left(\frac{2\pi R}{P}\right) & \text{describes the helix shape of a wire, illustrated by figure 5.4c} \\
r_j & \text{length from centre of the core wire,} \\
& \text{to the centre of a wire in the } j^{th} \text{ layer} \\
P & \text{helical pitch of the lay length} \\
E_j & \text{Young's modulus, denoted } j \text{ if composite configuration} \\
\nu_j & \text{Possion's ratio of a wire} \\
I_{w,j} = \frac{\pi \delta^4}{64} & \text{denotes the second moment of area of a wire} \\
A_{w,j} = \frac{\pi \delta^2}{4} & \text{denotes the cross sectional area of a wire}
\end{cases}
$$

(a) Hysteresis loop during bending.

(b) Stiffness curvature relation.
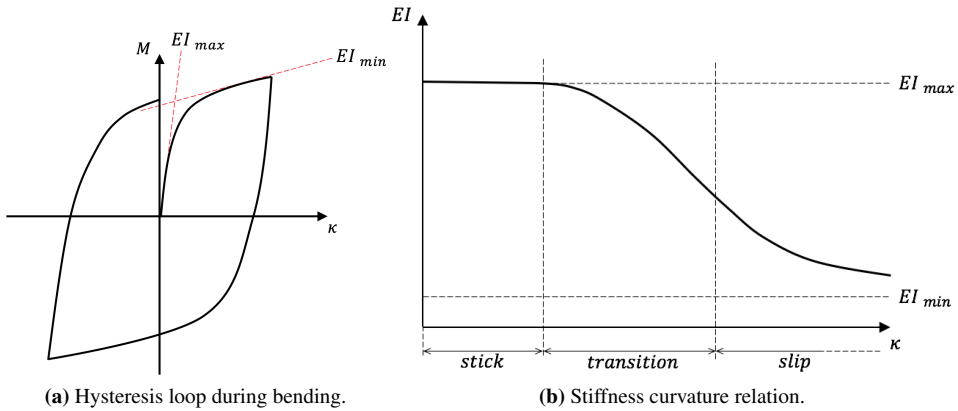
Figure 5.5: Stiffness-curvature relation of a cable subjected to bending.

As expressed by equation 5.8, the sum of inter-layer stick- and slip friction yields the maximum resistance to bending. Subsequently, whenever the sticking force is exceeded, a slip occurs and the resistance to bending decreases, this is illustrated in figure 5.5. The transition from stick to slip of the cable is smooth due to the inter-layer stick-slip effect of the wires, occurring at slightly different curvatures. However, one can assume that the bending stiffness of the cable always has its lowest possible value, given by the sum of its containing wires [27]. By applying these equations, one should obtain accurate estimates for the dynamic responses of a cable during simulations.

5.4 Pulley

A basic overview of the main forces occurring in a pulley is illustrated in figure 5.6, and expressed in order to describe its main contributions to the dynamic behaviour of a cable-pulley system. The inertia in a cable-pulley system becomes important when considering the dynamic behaviour as a whole. The rotation of the sheaves is purely caused due to frictional forces in a cable-pulley interaction. In cases of sudden surges, accelerations, and movement direction, e.g. wave compensation during offshore lifts or cable driven robotics. Several nonlinear effects may occur in the system, such as sliding, friction induced vibrations causing oscillations in cables, etc. In order to examine what may cause sliding between the contacting surfaces, one has to investigate both the static and dynamic characteristics. Considering the pulley illustrated in figure 5.6 as fixed (no rotation), the deviation of tensions on the verge of slipping is obtained by the Euler's equation [13, 31]

$$F_1 = F_2 e^{\mu\theta} \tag{5.9}$$

The force deviation over the pulley is purely due to friction effects that occurs, thus the frictional slipping force may be written in the form

$$\Delta F = F_{slip} = F_1 - F_2 \quad \Rightarrow \quad F_{slip} = F_1(e^{\mu\theta} - 1) \tag{5.10}$$
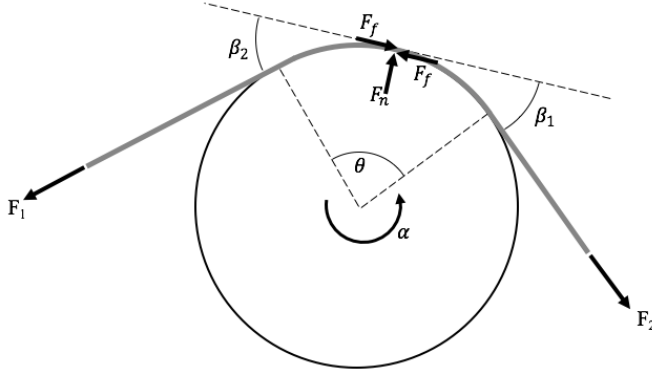
Figure 5.6: Analytic overview of a pulley.

Considering a pulley with a rotational mass with the moment of inertia J, a viscous damper constant B, angular displacement α, radius R, and the interaction cable-pulley friction force F_f, an equilibrium equation for the pulley yields [32]

$$J\frac{d^2\alpha}{dt^2} + B\frac{d\alpha}{dt} - F_f R = 0 \tag{5.11}$$

The frictional force is dependent on the contact force acting normal to the surface F_n, which can be simplified from a distributed to a concentrated load. The relation between the cable tension and frictional force F_f can be found through simple geometric analysis, and yields the angular relationship

$$F_n = F_1 \sin\beta_1 + F_2 \sin\beta_2 \tag{5.12}$$

with geometrical relations $\beta_1 = \beta_2$, $\beta_1 + \beta_2 = \theta$, and assuming $F_1 = F_2$, the relation can be rewritten as

$$F_n = F_1 \sin\theta \quad \Rightarrow \quad F_f = \mu F_2 \sin\theta \tag{5.13}$$

It is also worth noting that θ is the cables angular change of direction, as well as describing the arc over the pulley. If one is to consider when slipping occurs in dynamic situation, such that $F_f \geqslant F_{slip}$, by substituting equation 5.10 into 5.11, the relation is expressed as following

$$J\frac{d^2\alpha}{dt^2} + B\frac{d\alpha}{dt} \geqslant F_{slip}R \quad \Rightarrow \quad \frac{1}{R}\left(J\frac{d^2\alpha}{dt^2} + B\frac{d\alpha}{dt}\right) \geqslant F_1(e^{\mu\theta} - 1) \tag{5.14}$$

According to this equation, the limit between static and sliding friction are determined, and will further in this text be referred to as a frictional saturation force. If the saturation value is exceeded, i.e. when the inertial forces of the pulley exceeds static friction, slip occurs and the surfaces slide against each other.

5.5   Tribology

In general, virtually all mechanical systems involve some sort of interaction effects such as friction, heating, wear, etc. This well-known phenomenon which could affect the mechanical behaviour in one way or another. These effects are essential to study and evaluate in order to determine its level of impact on the overall performance, and possibly establish proper mathematical descriptions for improving the formulations of contact. However, some of these phenomenons exceed the framework of this study, but their importance will be touched upon. The topic of tribology in this text, confines to the dominating phenomena influencing the system behaviour, that is friction, referred to as the *stick-slip* effect.

5.5.1   Stick-slip friction

Contact forces involving friction in a cable-pulley interaction have been discussed. From now on static friction is referred to as *sticking* friction, and sliding will be called the *slipping* friction. This friction is considered to be a force that resists the relative movement between contacting surfaces, it is reasonable to argue that in an interaction between a cable and pulley, belt-drives etc. preventing relative movement ν_{sl} is a matter of interest.
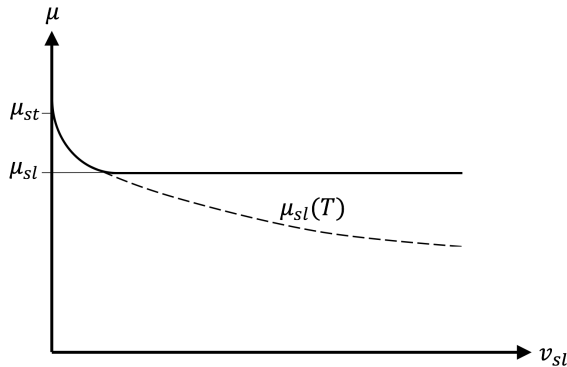
Figure 5.7: Conventional stick-slip curve.

The modes of stick and slip are described by static and dynamic coefficients of friction, μ_{st} and μ_{sl} respectively. And determines the force of saturation for sliding between objects.

5.5.2   Thermal effects

Friction-induced thermal effects is an existing phenomenon, which may affect the friction coefficients in certain scenarios. For instance, Peng et al. [33, 34] and Ma et al. [35] both addresses in recent articles the importance of studying the thermal effects due to the contacting pressure between a friction lining and wire ropes. Frictional heating causes the temperature between a wire and the groove to rise. This results in a reduction of the friction coefficient between the contacting pair of surfaces, illustrated by figure 5.7. If a load exceeds the friction, the velocity of sliding increases, which may cause fatal consequences in cases of emergency stops of cable-pulley systems, such as elevators, etc.

5.5.3 Friction induced vibrations

Friction is the primary source of vibrations in many mechanical systems, which may trigger unstable behaviour of system components [36], these oscillations are often associated with irregular dynamics [37]. If the friction coefficient is dependent on sliding velocity, and has a negative slope with respect to its velocity as shown if figure 5.7, it gives rise to negative damping. In this case, the friction may develop a so-called stick-slip motion which is governed by static and kinetic friction forces. Thus, contact forces between sliding surfaces may lead to strongly nonlinear, discontinuous and nonsmooth mathematical models [38].

5.5.4 Other frictional effects

(a) Frictionless case   **(b)** Frictional case
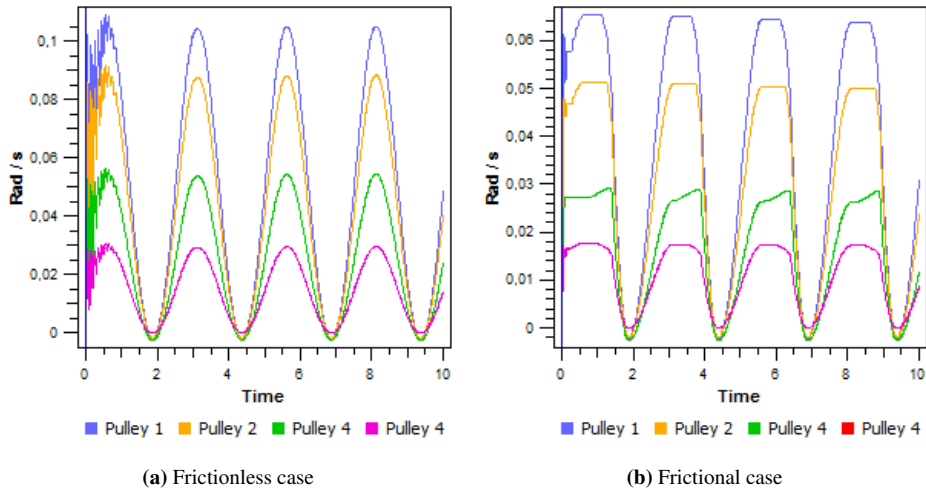
Figure 5.8: Comparison of displacements with and without stick-slip friction.

At the end of Section 5.2, effects caused by elastic storage of potential energy in a cable were mentioned, causing dynamic deformations of the cable. Another plausible scenario worth discussing, is how an oscillatory motion of the cable may affect the motion of the pulleys. As one can see in figure 5.8a, a harmonic load was applied to a system consisting of four pulleys. "Pulley 1" is attached at the tip of the crane boom, and "Pulley 4" at the innermost part of the boom. This data was obtained from a crane model in FEDEM, presented in Chapter 3. The elastic energy storage of the cables, combined with the variations of the oscillating pivot amplitudes of the sheaves, may trigger unstable behaviour of the system.

5.6 Structural dynamics

The dynamic behaviour of a supporting structure where a cable-pulley system is mounted, e.g. a crane. The dynamics are vital to study and evaluate, for instance, the stiffness properties of a crane may vary with respect to its position. Structural properties such as different mode shapes and its associated frequencies also need to be surveyed. The mounting structure itself is critical for how the dynamics of a cable-pulley system evolves during an operation. When preforming simulations and analyses of dynamic systems, it is normal to determine the natural frequencies and mode shapes as a first step. The obtained results are important for describing the basic dynamic behaviour of a structure and provides an indication of its responses to dynamic loading. There are several reasons for computing natural frequencies and its associated mode shape, an interest in a case such as this one is to assess the dynamic influence between a pulley and its supporting structure. A second order expression of equations for an arbitrary structure can be written

$$\mathbf{M\ddot{r}} + \mathbf{C\dot{r}} + \mathbf{Kr} = \mathbf{Q}(t) \tag{5.15}$$

In order to evaluate the natural frequencies, the damper matrix $\mathbf{C}$ and external loads $\mathbf{Q}(t)$ is neglected. Thus, the remaining equation expressed by mass $\mathbf{M}$, acceleration $\mathbf{\ddot{r}}$, stiffness $\mathbf{K}$ and displacement $\mathbf{r}$, yields

$$\mathbf{M\ddot{r}} + \mathbf{Kr} = \mathbf{0} \tag{5.16}$$

with the assumption of oscillating behaviour is of simple harmonic sinusoidal character

$$\mathbf{r} = \boldsymbol{\phi} \sin \omega t \quad \Rightarrow \quad \mathbf{\ddot{r}} = -\omega^2 \boldsymbol{\phi} \sin \omega t \tag{5.17}$$

Substituting equation 5.17 into 5.16 one obtains the dynamic properties of the system

$$(\mathbf{K} - \omega^2 \mathbf{M})\boldsymbol{\phi} \sin \omega \mathbf{t} = \mathbf{0} \quad \Rightarrow \quad (\mathbf{K} - \omega^2 \mathbf{M}) = \mathbf{0} \quad \Rightarrow \quad \omega_n = \sqrt{\frac{k}{m}} \tag{5.18}$$

where ω denotes the natural frequency and $\boldsymbol{\phi}$ its corresponding mode shape. If it is chosen to implement the cable-pulley in an in custom designed program, it is essential to implement the dynamics of its supporting structure.

5.7 An accumulation of dynamic effects

Considering an accumulative scenario of extremes, where all the presented effects contribute to an amplification of out of phase tension in a cable-pulley system. Thus, all the presented effects contributes to an amplification of out of phase tension in a cable-pulley system. As of noted in Section 5.2, if unwanted frequency vibrations exhibit in a system, the cables will deform dynamically, storing energy like a spring. Considering a scenario where friction-, damper- and inertia effects of the sheaves become significant, in a resonant stage, the pulleys may be subjected to oscillations that are in counter-phase, causing a cable to jump off. Thus, the importance of including these effects will be a foundation

when evaluating different elements in the following chapter. As demonstrated in Chapter 4, the approaches for describing these effects are diverse, and their integrity varies.

Chapter 6

Investigated elements

A vast amount of finite elements has been developed over the years, often for specific objectives and purposes. Problems involving simulations of flexible multibody systems e.g. cable and pulleys, possibly mounted on another dynamic support structure such as a crane, is extremely nonlinear in its nature. Systems like these are often referred to in the FEM world as multibody systems, further discussed in the following chapters. Such systems often tend to become large and complex, mainly consisting of mathematical models containing large sets of nonlinear differential equations, thus, the computational cost increases, making it time consuming.

In order to identify a suitable element, further for a digital twin application, computational cost becomes critical. Exact rigid body motion of an element is also essential when working with flexible objects in multibody dynamics that are undergoing large reference displacements.

This chapter provides a rapid review of elements which may be used for this purpose, a comparison will be carried out in order to identify their strengths and weaknesses, and for obtaining a conclusion.

6.1 A finite element of cable passing through a pulley (FECP)
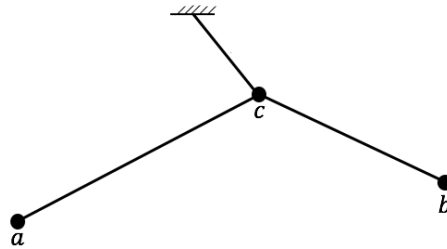
Figure 6.1: Cable-pulley element.

A finite element of a cable passing through a pulley of great conceptual simplicity was suggested by Aufaure [39]. The element was intended for investigating the deformation of electric cables passing through pulleys as figure 6.1 illustrates. The derivation was based on the assumptions of a perfectly elastic cable, the supporting pulley is able to roll along the cable, but must not reach the endpoints. Another simplification was to consider equal tensions in the cable segments ab and cb, neglecting friction. The two segments of the cable ac and cb remain rectilinear during the simulation, like a two-node first-order cable element.

6.2 Slipring connector (SRC)
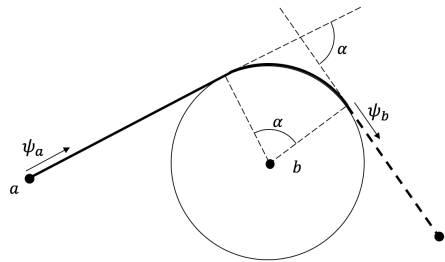
Figure 6.2: Slipring connector.

Abaqus is using an element called the *Slipring connector* , inter alia for describing pulley and taut cable systems [40]. Instead of constraining any components of relative motion, the elements of the system are defined to be at rest. Instead a so-called *material flow* Ψ degree of freedom is introduced and mimicks how a cable passes through the system. The radii of the pulley is neglected in this formulation, and the friction force between the cable and pulley is defined by the angle and a friction coefficient. If a cable element is to be modelled between node a and b, the material flow is introduced as Ψ_a and Ψ_b. The material flow can pass rigidly through the element without stretching, stretching can occur with no flow, and both cases can occur simultaneously.

6.3 The bar finite element for cable (BFEC)

The bar finite element [41] is based on a common approach for modelling a rope and cables. The principle is to split it into bar elements which are considered as perfectly straight, homogeneous with elastic properties, and neglecting the rotational DOFs. However, in this formulation, bending stiffness is included, although it is not defined by the element properties, but through a couple between consecutive bar elements. These leads to forces on the extremities of these two elements when a curvature occurs on the modelled cable. In order to obtain an exact representation of a cable, a large amount of elements are necessary.

6.4 Super element approach (SEA)

Ju and Choo [13] proposed an approach for modelling how a cable passes through a set of pulleys by means of super elements for large cable-pulley systems. The authors addressed in this work that friction-free and fixed models provides unrealistic and incorrect results of how the tensions dissipate in cables through a system. Thus further induce inaccurate behaviour when simulating its supporting structure. The super element was established and expressed by sub-elements, modelled as a cable passing through a pulley, the pulley is considered as a node, neglecting its physical behaviour. The cables were considered as linear tensile elements, where the alteration of tension over the pulleys are described by the *Euler's friction law*. This is expressed by the angle of change in direction and its friction coefficient, or empirical relations as a "loss-coefficient". When working with large systems that contain a continuous cable which loops around and passes through multiple pulleys. Such systems are used in heavy lifts, in such cases the pulleys directly attached to a structure were considered supernodes. This element has the ability to distribute forces in a cable over long distances of complex geometric paths, providing a good representation of its structural impact.

6.5 Floating frame of reference (FFR)

The *floating frame of reference* formulation is a widely used methodology in flexible multi-body dynamics [42, 43, 44, 45]. In problems involving three-dimensional beam deformation, one needs to carefully consider its motion. The classical *Euler-Bernoulli* beam assumptions is inadequate for completely describing the displacement of its centerline. For instance, a vector describing the position of a centerline during rigid rotational displacement of a beam will remain constant during its motion [46]. To deal with this problem the configuration of the FFR uses two sets of coordinate systems; the first set describes the position and orientation of the body, while the second set describes deformations of the body with respect to it. These two coordinate systems are referred to as the *reference* or *global* coordinate system and the *elastic* or *local* coordinate systems [42, 47]. Thus, leading to an exact representation of rigid body motion, satisfying the criterion of zero strain in the element during an arbitrary rigid body motion.

6.6 Nodal position formulation (NPFEM)

The element properties of the nodal position formulation derived by Sun et al. [18] is similar to a conventional two-node bar element. The main difference is that the components of longitudinal stiffness has a scaling factor $\frac{L}{L_o}$ yielding $\frac{EAL}{L_o^2}$. The stiffness matrix of the cable in the global coordinate is defined $\mathbf{K} = \mathbf{Q^T K_0 Q}$, where $\mathbf{K_0}$ denotes the local stiffness matrix and $\mathbf{Q}$ is the coordinate transformation matrix from local to the global coordinate system. In addition, the NPFEM yields an extra equivalent nodal elastic force vector which does not exist in other element formulations, $\mathbf{F_k} = EAL\mathbf{Q^T B_0^T}$, where $\mathbf{B_0}$ denotes the strain matrix. This is not an external force but a result of the transformation from state variables of nodal displacements to nodal positions, and is a function of the element rigidity EA and the orientation. Since the coordinate transformation matrix of the cable element $\mathbf{Q}$ varies with time, $\mathbf{K}$ and $\mathbf{F_k}$ are highly nonlinear and time dependent.

6.7 Geometrical nonlinear beam formulation (GNBF)

Jonker and Meijaard [48] derived a finite element beam, designed for simulating flexible multibody systems that undergo large deflections. The beam is described as a shear deformable element that is expressed through a *discrete deformation mode formulation*. The modes are characterised by deformation coordinates also known as generalised deformations related to conventional small-deflection beam theory. The formulation is based on the well-known *Timoshenko beam theory*, but includes geometric non-linearity that account for large deformations, buckling, and post-buckling, by introducing additional second-order terms in the expression of deformation modes.

6.8 The absolute nodal coordinate formulation (ANCF)

This formulation is based on *Euler-Bernoulli beam theory*, and was first proposed by Shabana [42] with the intent for an element that can be used in analyses of flexible bodies undergoing arbitrary displacements involving large rotational deformations. This formulation expresses the degrees of freedom as the absolute nodal positions and slopes, for interpolation of the position field of the beam element, instead of infinitesimal or finite rotations of the nodes. Thus, an arbitrary point at the centerline of a two-node element is expressed $\mathbf{r}(\xi) = \mathbf{S}(\xi)\mathbf{e}$, where $\mathbf{S}(\xi)$ is an interpolation matrix containing the shape functions expressed by the classical *cubic Hermite polynomials*, and $\mathbf{e}$ the global positions and slopes. The formulation is based on a continuum mechanics approach that describes the displacement field when deriving its elastic forces. This element allows large deformations and has an exact description of rigid body displacements. One of the most important features the element inherits is the constancy of its mass matrix, which makes it efficient when solving for accelerations, but on the expense of centrifugal and Coriolis forces. However, it has been reported by several authors that the formulation suffers from locking effects.

Locking effects demonstrated

A shear deformable Timoshenko beam element has the stiffness matrix [49]:

$$\mathbf{K} = \frac{EI}{\alpha L} \begin{bmatrix} k_{11} & k_{12} & \cdots & k_{ij} \\ k_{21} & \ddots & & \\ \vdots & & \ddots & \\ k_{ji} & & & k_{jj} \end{bmatrix}, \qquad \text{where} \qquad \alpha = \frac{12\kappa EI}{GAL^2} = 2\left(\frac{h}{L}\right)^2 \tag{6.1}$$

$$\text{If} \quad \frac{h}{L} \to 0 \quad \text{then} \quad \alpha \to 0 \quad \text{and} \quad \mathbf{K} \to \infty$$

Here, α is a dimensionless shear parameter. L is the length of a beam, and h its thickness. When the length-thickness ratio decreases, the shear effects will dominate the stiffness more and more. If the length-thickness ratio approaches zero, the stiffness matrix tends to blow up [49].

6.9 Modifications of the ANCF

As mentioned, the reported locking problems have been addressed in the literature which have mobilised multiple scientists [16, 50, 51, 52] for handling these phenomenons. In these articles, the proposed formulations has resulted in several modifications of the ANCF beam. In order to eliminate the locking effects, the beam formulations are enhanced by a term accounting for the thickness. Thus the formulation treats the element as a volume instead of a beam. By doing so, a second interpolation variable was introduced, extending the interpolation terms. Thus, an arbitrary material point in the beam is expressed as $\mathbf{r}(\xi, \eta) = \mathbf{S}(\xi, \eta)\mathbf{e}$. There are some differences between these formulations:

- **Dufva et al. (ANCF - Du)** Dufva et al. [16] were the first to propose an element that uses the original shape functions for interpolating the bending curvature, while introducing a linear interpolation function for the describing shear deformation.

- **García-Vallejo et al. (ANCF - GV)** Gracía-Vallejo et al. [51] suggested an augmented formulation of the ANCF beam by means of introducing a third node in the element with modified polynomial expansions. This, alone did not eliminate the shear locking problems, and a reduced integration procedure was introduced.

- **Nachbagauer et al. (ANCF - Na)** Nachbagauer et al. [52] had a similar approach to Dufva et al. but suggested two formulations of the element. In the first formulation, linear interpolation functions were applied. Thus, the second formulation applied quadratic interpolation functions to describe bending, and linear functions for describing shear.

- **Von Dombrowski (ANCF - VD)** Von Dombrowski [50] introduced an element based on the ANCF in order to cope with the absence of centrifugal and Coriolis forces on the expense of the constant mass matrix.

6.10   Comparison and discussion

In order to determine the most suitable formulation, a *full consensus prioritization matrix* normally applied during product development, is used for comparing the elements against each other. Certain criteria was created to help compare the elements to each other, this is shown in the following:

- **Decency:**   Ability to portray the physical effects discussed in Chapter 5.

- **CPU cost:**   Computationally cost efficient for a digital twin application.

- **Verification:**   Experimentally verified with physical tests.

- **Recognition:**   Establishment and acknowledgement in other literatures.

- **Complexity:**   The mathematical complexity of the beam formulation.

The methodology is carried out in two steps, first, prioritise the criteria and determine the total *weight if priority*, this is illustrated in figure 6.3a. Second, evaluate the different elements ability to cope alone with the given criteria. The total integrity of the elements are illustrated in figure 6.3b.

(a) Weight of priority   **(b)** Summary
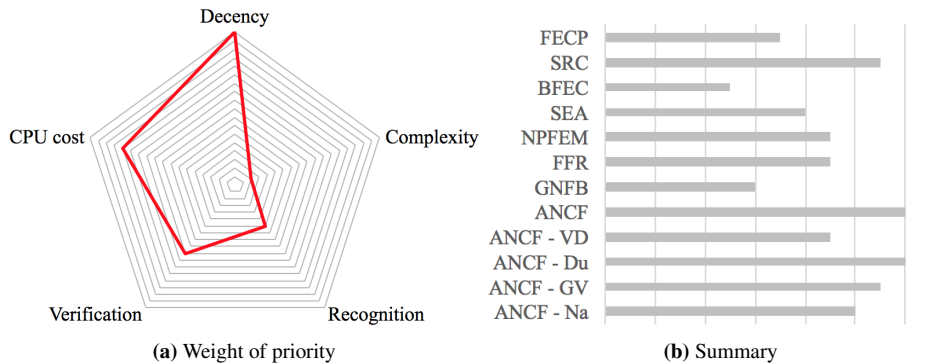
Figure 6.3: Graphical illustration of element criteria and objective outcome

Element	Decency	Complexity	Recognition	CPU cost	Verification
FECO	Poor	Excellent	Fair	Excellent	Poor
SRC	Fair	Excellent	Excellent	Excellent	Good
BFEC	Poor	Good	Fair	Fair	Fair
SEA	Fair	Good	Poor	Excellent	Fair
NPFEM	Fair	Good	Poor	Excellent	Good
FFR	Good	Good	Excellent	Poor	Excellent
GNBF	Good	Poor	Poor	—	Poor
ANCF	Excellent	Good	Excellent	Good	Excellent
ANCF - VD	Good	Good	Good	Fair	Good
ANCF - Du	Excellent	Good	Good	Excellent	Good
ANCF - GV	Excellent	Good	Good	Fair	Good
ANCF -Na	Good	Good	Fair	Excellent	Fair

In order to determine which element to use, one needs to consider it for the purpose. In structural or more quasi-static problems, the slipring or the super element approach, is an agreeable simplification for large construction problems where the dynamics of cable-pulleys itself is not a direct area of interest, but rather their impact on the overall behaviour of a support structure. However, if the inherent dynamics of a cable pulley system itself is the field of interest, these simplifications is not satisfactory for capturing the exact behaviour of a system, thus are disqualified for the purpose of this research.

Also, the NPFEM and BFEC formulation for describing a cable is inadequate for the purpose of this development, due to the incapability for describing bending.

The FFR formulation is maybe one of the most commonly used elements for describing flexible objects in multibody systems. However, FFR is very confined to small deformations, resulting in a very large amount needed in comparison to those who use absolute coordinates. Also, the coupling between the reference motion and its elastic deformation leads to a highly nonlinear mass matrix. Thus, it is not applicable for modelling and simulation of objects subjected to large deformations, inter alia cable elements.

The GNBF element was recently introduced and has not yet been recognised in other literature. Its formulation is also found to be complicated but seems to provide adequate performance, yet, the author does not mention anything about its computational expenses.

The ANCF has been recurring during the review of different literature concerning cables, ropes and slender beam like objects. In all literature that apply the ANCF, the element are subjected to large deformations, and has been proving good results [12, 20, 23, 24]. It is also referred to as a good option in literature's of researchers that uses other formulations [18]. However, problems regarding locking effects have been mentioned by several authors. This mobilised scientists to develop elements that cope with such problems, resulting in modified ANCF formulations.

Next to the original formulations, the modified ANCF elements are considered to be strong candidates, the authors argues for their elements to be more suited for tasks involving highly nonlinear deformations.

Nachbagauer et al. emphasises in their literature that the proposed element is computationally more efficient because it requires less integration points. This is due to the fact that it has lower order formulations, compared with the original element. It is also pointed out that its convergence is faster in the iteration process. However, this element applies linear and quadratic shape functions, that implies the need of a larger amount of elements to obtain an equal representation of contact forces as the original one.

By introducing a third node, as García-Vallejo et al. suggested the DOFs are increased by fifty percent, but applies a reduced integration scheme that reduces the computational expenses. However, by the introduction of reduced integration, other complications occur that needs to be taken into account, such as so-called *hour-glass* effect.

The element introduced by Dufva et al. is the one considered as the strongest candidate to the original ANCF. Unfortunately, only a two-dimensional version of this element formulation was found.

However, the effects of locking are reported to occur in stiff beams [53], and has proven to provide adequate simulations for rope-like objects in recent literature [20, 21, 22, 24], and often chosen for its simplicity of derivation. Also, the author considered the modified ANCF elements as immature due to the lack of experimental verification through

physical comparison and recognition in literature provided by other scientists, and has, therefore, put these on hold. The original ACNF was also chosen due to the successful results that Bulín et al.[24] provided in their recent work. It has also been subject to extensive development during the last two decades and has started gaining recognition and integrity in the field of flexible multibody dynamics, hence there is more literature supporting this formulation for the application of cable-pulley systems, i.e. rigid-flexible multibody dynamics.

Chapter 7

Mathematical modelling of a cable and a pulley

Multibody systems generally include two collections of bodies, one consists of compact and bulky bodies, while the other includes typical structural components such as rods, beams, plates, and shells. Rigid bodies have a finite number of DOFs, a planar rigid body has three, two translational and one rotational. On the other hand, structural components have an infinite number of DOFs that describe the displacements of an arbitrary point on the components that are obtained through interpolation [54].

7.1 The absolute nodal coordinate formulation

The *absolute nodal coordination formulation (ANCF)* is a relatively new approach, and was first proposed by Shabana [19]. Among other things, the ANCF elements have mainly been developed for the simulation of flexible multibody dynamics in particular [42, 47, 55], and is a non-incremental finite element procedure [56]. The element is consistent with the nonlinear theory of continuum mechanics, and easy to implement. It has been widely used for more than a decade in research topics investigating the dynamics of flexible bodies that is subjected to large rotations and deformations [53]. Several researches that has investigated challenges related to the issue of cable-pulley dynamics, some more than others, has applied this formulation in their research with a conform opinion of promising results [12, 15, 20, 22, 24, 53]. The basic concept for the ANCF methodology is to use absolute positions for the nodes (reference vectors) and slopes (reference vector derivatives) as a set of nodal coordinates. Thus, it utilises global slopes and absolute displacements, instead of infinite small or finite rotations to define the element coordinates. The deformations and locations of the material points in the element are therefore defined in the global coordinate system through nodal coordinates, and an interpolation matrix containing the element shape functions. In order to distinguish, these are called *global shape functions*, and are not equal to the local shape functions used in more conventional elements such as the FFR. Due to this formulation, the position of an arbitrary material point in the element is described by means of interpolations based on the Cartesian absolute coordinates of the nodal points, and the positions gradient with respect to material coordinates containing a reference configuration [42].

There are some important fundamental differences between the ANCF and the classical FFR formulation. Due to its usage of global positions and slopes, it results in a large amount of DOFs, if a spatial beam is considered, it contains 24 nodal DOFs, instead of 12 for a conventional two-node beam element. Another difference is the formulation of its stiffness matrix that is highly nonlinear in the case of ANCF, even in the case of simple linear elastic models. The nature of the coordinates used in the ANCF does not include infinitesimal or finite rotations. Also, the coordinate transformation in order to determine the element mass matrix is not needed , the mass matrix also remains constant which makes it computationally more efficient compared with other nonlinear formulations. Thus, attention must be paid when defining the generalised forces associated with the global slopes of the element [47].

7.1.1 Two-dimensional formulation of an ANCF beam element

The ANCF planar beam was first introduced by A.A Shabana in 1997 [19], and was adapted to a spatial formulation in 2001 [46]. For simplicity, the planar formulation is presented in this section. A three-dimensional element is completely equivalent with the two-dimensional formulation, it only requires implementation of the z-coordinate in the cross-section of the beam, and the absolute nodal coordinates [19].

The FE-model of the cable is modelled as a planar ANCF beam, as illustrated in figure 7.1, and consists of two nodes, and with the length l. An arbitrary point on the neutral axis of the beam can be expressed in global coordinates $\mathbf{r} = [r_x, r_y]^T$ in the following formulation:
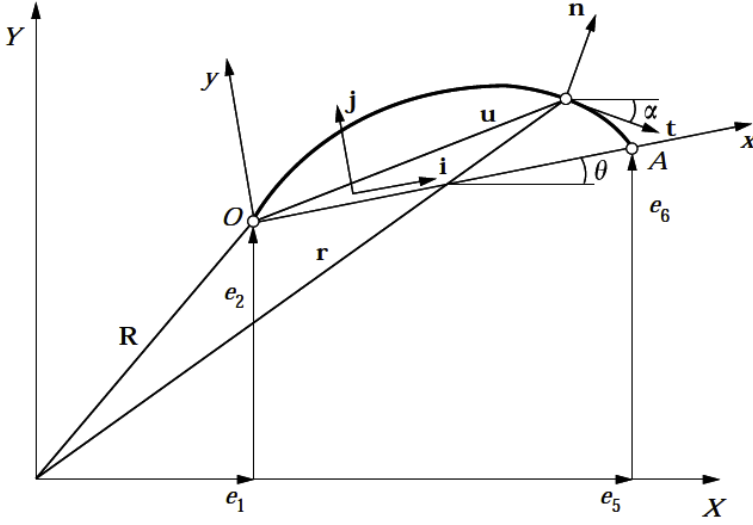
Figure 7.1: A planar ANCF beam element [47].

$$\mathbf{r} = \mathbf{Se} \quad , \quad \mathbf{e} = [e_1 \ e_2 \ \cdots \ e_8]^T \tag{7.1}$$

The global positions $\mathbf{r}$ can be calculated my means of interpolation matrix $\mathbf{S}$ and the vector of nodal variables $\mathbf{e}$. Matrix $\mathbf{S}$ and vector $\mathbf{e}$ is also known as *the matrix of global shape functions* and the *vector of nodal coordinates* respectively. In the vector of nodal coordinates $\mathbf{e}$, the translation coordinates of the node at O is given by e_1 and e_2, likewise, e_5 and e_6 describes translation of node A. The curvature of the element is given by e_3 and e_4 that describes the slope at O, along with e_7 and e_8 at A. Thus, the absolute coordinates are expressed as follows

$$
\begin{aligned}
e_1 &= r_x(x = 0) & e_2 &= r_y(x = 0) \\
e_3 &= \frac{\partial r_x(x = 0)}{\partial x} & e_4 &= \frac{\partial r_y(x = 0)}{\partial x} \\
e_5 &= r_x(x = l), & e_6 &= r_y(x = l) \\
e_7 &= \frac{\partial r_x(x = l)}{\partial x}, & e_8 &= \frac{\partial r_y(x = l)}{\partial x}
\end{aligned}
\tag{7.2}
$$

The shape function matrix $\mathbf{S}$ contains a complete set of rigid body modes which describes arbitrary translational and rotational displacement patterns of the element. These modes corresponds with the associated displacements of the nodes, e_1, e_2 with s_1 ,, e_3, e_4 with s_2, and so on. The shape functions are defined by the *cubic Hermite polynomials* as

$$
\begin{aligned}
s_1 &= 1 - 3\xi^2 + 2\xi^3, & s_2 &= l(\xi - 2\xi^2 + \xi^3), \\
s_3 &= 3\xi^2 - 2\xi^3, & s_4 &= l(\xi^3 - \xi^2),
\end{aligned}
\tag{7.3}
$$

Where $\xi = \frac{x}{l}$.
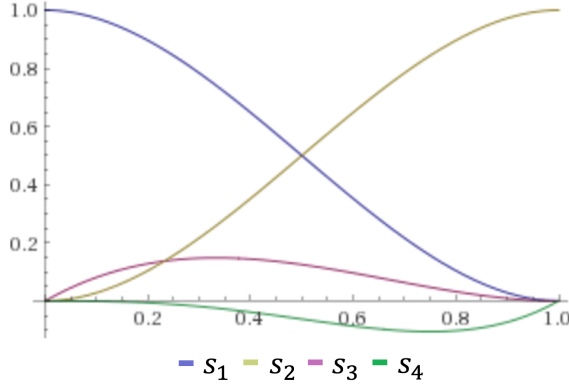
Figure 7.2: Cubic Herimite polynomials.

$$\mathbf{S}(\xi) = \begin{bmatrix} s_1\mathbf{I} & s_2\mathbf{I} & s_3\mathbf{I} & s_4\mathbf{I} \end{bmatrix}, \qquad \mathbf{I} = \begin{bmatrix} 1 & 0 \\ 0 & 1 \end{bmatrix} \tag{7.4}$$

The global shape functions $\mathbf{S}(\xi)$ are independent of time, and the nodal coordinates $\mathbf{e}$ independent of ξ, while dependent on time in dynamic simulations.

$$\mathbf{r}(\xi, t) = \mathbf{S}(\xi)\mathbf{e}(t) \tag{7.5}$$

Thus, the time derivatives are

$$\dot{\mathbf{r}}(\xi, t) = \mathbf{S}(\xi)\dot{\mathbf{e}}(t) \tag{7.6}$$

$$\ddot{\mathbf{r}}(\xi, t) = \mathbf{S}(\xi)\ddot{\mathbf{e}}(t) \tag{7.7}$$

The cross-section of the element is assumed to remain plane and perpendicular to the neutral axis during deformation. The longitudinal strain ε is described by the *Green-Lagrange longitudinal Strain Tensor*

$$\varepsilon = \frac{1}{2}(\mathbf{r'}^T\mathbf{r'} - 1), \tag{7.8}$$

And the curvature of the beam κ derived from the *Euler-Bernoulli beam theory*

$$\kappa = \left| \frac{d^2\mathbf{r}}{ds^2} \right| = \frac{|\mathbf{r''} \times \mathbf{r'}|}{|\mathbf{r'}^3|}, \qquad ds = \sqrt{\mathbf{r'}^T\mathbf{r'}}d\xi \tag{7.9}$$

where $\mathbf{r'}$ and $\mathbf{r''}$ is the derivative with respect to x. In order to obtain a mathematical model that describes the characteristics of the ANCF beam element, the principle of virtual work is applied i.e. *Lagrange's equation*. Thus, the strain energy of longitudinal deformation E_t, and the strain energy contributed by bending E_b are expressed as follows

$$E_{\mathrm{p}} = E_t + E_b = \frac{1}{2} \int_0^l \left(EA\varepsilon^2 + EI\kappa^2 \right) ds \tag{7.10}$$

As of noted in Section 5.3, the author suggests to incorporate the minimum bending stiffness obtained from equation 5.7. This will obtain realistic bending characteristics of a cable. Also, scaling the modulus of elasticity E by a factor of 0.9 to obtain more realistic elastic responses in the longitudinal direction of a cable is reasonable [57]. Thus, the modified expression of strain energy of an element with sub-index n has the form

$$E_{\mathrm{p}} = E_t + E_b = \frac{1}{2} \int_0^l \left(0.9EA\varepsilon^2 + EI_{min}\kappa^2 \right) ds = \frac{1}{2} \mathbf{e}_n^{\mathbf{T}} \mathbf{K}_n \mathbf{e}_n \tag{7.11}$$

where $\mathbf{K}_n$ denotes the stiffness matrix of an element. By introducing these parameters, the element becomes capable of presenting a high stiffness in axial direction, yet opposing a small resistance to bending, as a typical cable. Furthermore, accounting for the kinetic energy of the element with material density ρ, has the following expression

$$E_{\mathrm{k}} = \frac{1}{2} \int_V \rho A \dot{\mathbf{r}}^T \dot{\mathbf{r}} dV = \frac{1}{2} \dot{\mathbf{e}}^T \int_V \rho A \mathbf{S}^T \mathbf{S} dV \dot{\mathbf{e}} = \frac{1}{2} \dot{\mathbf{e}}_n^{\mathbf{T}} \mathbf{M}_n \dot{\mathbf{e}}_n \tag{7.12}$$

yielding the mass matrix of the element $\mathbf{M}_n$. The results obtained in equation 7.12 and 7.10 are introduced to *Newtons second law*. Thus, the equation of motion of an element are obtained in a matrix form as follows

$$\mathbf{M}_n \ddot{\mathbf{e}} + \mathbf{K}_n \mathbf{e}_n = \mathbf{Q}_n \tag{7.13}$$

where $\mathbf{Q}_n$ is a vector containing a set of generalised nodal forces. Due to the nonlinear characteristics of stiffness matrix $\mathbf{K}_n$, and constancy of mass matrix $\mathbf{M}_n$, it is beneficial to consider $\mathbf{K}_n$ as a part of the external forces i.e. the elastic forces. Thus, equation 7.13 can be written in the term [58]

$$\mathbf{M}_n \ddot{\mathbf{e}}_n = \mathbf{Q}_n - \mathbf{K}_n \mathbf{e}_n \tag{7.14}$$

The vector containing all the absolute nodal coordinates describes the entire configuration of the beam, are expressed as

$$\mathbf{e}(t) = \begin{bmatrix} \mathbf{e}_0(t)^T & \mathbf{e}'_0(t)^T & \mathbf{e}_1(t)^T & \mathbf{e}'_1(t)^T & \cdots & \mathbf{e}_n(t)^T & \mathbf{e}'_n(t)^T \end{bmatrix}^T \tag{7.15}$$

And the vector that describes an arbitrary point along the centerline of a beam configuration, expressed as

$$\mathbf{r}(t) = \begin{bmatrix} \mathbf{r}_0(t)^T & \mathbf{r}'_0(t)^T & \mathbf{r}_1(t)^T & \mathbf{r}'_1(t)^T & \cdots & \mathbf{r}_n(t)^T & \mathbf{r}'_n(t)^T \end{bmatrix}^T \tag{7.16}$$

i.e. the position of the beam elements and their gradient is specified at the nodes. A beam with n elements contain $n + 1$ nodes.

By introducing the matrix $\mathbf{C}$, which contains damper properties of the system, a beam assembled by n elements can therefore be expanded to the following expression.

$$\mathbf{M}_f\ddot{\mathbf{e}} = \mathbf{Q} - \mathbf{C}\dot{\mathbf{q}} - \mathbf{K}\mathbf{e} \tag{7.17}$$

$\mathbf{C}$ denotes a mass stiffness proportional damping matrix, with the mass- and stiffness proportional coefficients α and β which is often referred to as *Rayleigh damping*, and has the form $\mathbf{C} = \alpha\mathbf{M} + \beta\mathbf{K}$. Finally, all the contributions from external-, damping- and elastic forces can be written as a unified matrix of external forces, and has the following form

$$\mathbf{M}_f\ddot{\mathbf{e}} = \mathbf{Q}(\mathbf{e}, \dot{\mathbf{e}}, t) \tag{7.18}$$

As of noted, this formulation includes constancy in the mass matrix, at the same time it accounts for rotary inertia, shear, and torsion for spatial configurations, yet results in an absence of centrifugal and Coriolis forces. Mass constancy is an important feature, since most existing element formulations for nonlinear simulations that covers large rotations, includes incremental procedures and requires large vectors of rotation. Thus, the constant mass matrix enables efficient properties when solving for accelerations, if objects are modelled by the ANCF.

The formulation also leads to an isoparametric element which is beneficial in analyses of curved bodies. It does not require interpolation of finite rotation coordinates, instead, one can simply describe the same configuration through different sequences of orientation coordinates [46]. Thus, yielding the advantage of simplicity for detecting contact with other objects [15]. Simulation experiments have shown that displacement-based finite elements that do not employ rotations such as Euler angles, do not have numerical instabilities compared with those who have [55].

Also, a minimal set of nonlinear constraint equations are required when assembling beams of this formulation into a system containing rigid bodies defined by *natural coordinates*, and the equations of motion can be preserved [56]. It is also worth noting that if one assumes linear deformation in the moving frame, it allows for coordinate reduction by applying the CMS algorithm (see Section 3.1.1) [58].

Although, the ANCF element is able to describe the shear and cross-sectional deformations of a beam element, it suffers from locking problems, as discussed in Chapter 6. However, these effects deteriorate especially in problems where the beam inhere significant bending stiffness [53], that is not our case.

7.2 Defining a pulley by natural coordinates

For the modelling of systems that consist of both flexible and rigid links, fully-Cartesian coordinates, also known as *natural coordinates*, is a method compatible with the ANCF that can be used for building the system [56]. Natural coordinates are fully composed by Cartesian variables of certain unit vectors for describing the motion of a body, it does not include angular coordinates. It is therefore easy to define constraint equations, and easy to program [59, 60]. It is reasonable to consider a pulley as rigid in comparison with a cable. Defining a rigid body, r, with natural coordinates includes global position vectors
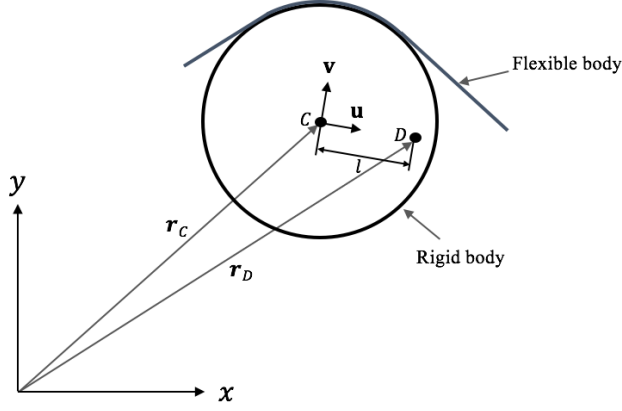
Figure 7.3: A rigid-flexible multibody system.

$(\mathbf{r}_C, \mathbf{r}_D)$ of minimum two basic points (C, D), and global unit vectors $(\mathbf{u}, \mathbf{v})$. The basic points relate to mass and stiffness properties, thus preferred to define an amount that are adequate for describing the inertia of a pulley. For two dimensional motion of a rigid body, a vector of coordinates that contain position vectors of its basic points, are described as follows:

$$\mathbf{d}_r = \begin{bmatrix} \mathbf{r}_C & \mathbf{r}_D \end{bmatrix}^T \tag{7.19}$$

The rigid body must fulfil the constant distance constraint, as the basic points are dependent on each other [60].

$$\Phi = \mathbf{d}^T \hat{\mathbf{I}} \mathbf{d} - l^2, \qquad \hat{\mathbf{I}} = \begin{bmatrix} \mathbf{I}_2 & -\mathbf{I}_2 \\ -\mathbf{I}_2 & \mathbf{I}_2 \end{bmatrix} \tag{7.20}$$

Defining its local coordinate system containing the unit vectors $\mathbf{u}$ and $\mathbf{v}$ composed of Cartesian coordinates

$$\mathbf{u} = \frac{1}{l}(\mathbf{r}_C - \mathbf{r}_D), \qquad \mathbf{v} = \frac{1}{l}\tilde{\mathbf{I}}_2(\mathbf{r}_C - \mathbf{r}_D) \tag{7.21}$$

where $\tilde{\mathbf{I}}_2$ is a skew symmetric matrix.

$$\tilde{\mathbf{I}}_2 = \begin{bmatrix} 0 & -1 \\ 1 & 0 \end{bmatrix} \tag{7.22}$$

For defining the natural coordinate system, the unit vectors are assembled into a rotation matrix $\mathbf{A}$, the motion described by these coordinates is a linear function.

$$\mathbf{A} = \begin{bmatrix} \mathbf{u} & \mathbf{v} \end{bmatrix} \tag{7.23}$$

In order for the rigid body to mimic the behaviour of a pulley, mass needs to be added to the basic points, and the equation of motion for a pulley r yields

$$\mathbf{M}_r\ddot{\mathbf{d}} + \mathbf{\Phi}_{\mathbf{d}}^T\boldsymbol{\lambda}_r = -\mathbf{Q}_c\,, \qquad \mathbf{\Phi}(\mathbf{d},t) = 0 \tag{7.24}$$

Here, $\mathbf{\Phi}_{\mathbf{d}}$ denotes the Jacobian matrix for the constant distance constraints, containing all the partial derivatives with respect to the body coordinates. $\boldsymbol{\lambda}_r$ is a vector of Lagrange multipliers, further explained in Chapter 9. The external forces, is in this particular case expressed as contact forces $\mathbf{Q}_c$, established in Chapter 8. The external forces might also be expressed as an applied torque, emulating an external power source.

It is reasonable to consider the pulley(s) as rigid, however, its supporting structure is most likely not, and may be subjected to deflections and large motions. Instead of implementing this formulation to an existing software, an alternative is to extract the mechanical characteristics of the structure from a FE-program for a given point, i.e. where a pulley is mounted. In order to do so, one can adapt the idea of supernodes, hence there is no "internal DOFs" to eliminate (see Section 3.1.1 or Sivertsen (2001) [8]). Denoting stiffness and eigenvectors to a pulley fixation $\mathbf{r}_C$, the structural characteristics obtained in Section 5.6 are applied.

$$\mathbf{r}_C = \boldsymbol{\phi}\sin\omega t \tag{7.25}$$

This introduces additional DOFs to the system, together with its corresponding stiffness matrix $\mathbf{K}_s$, obtained from its support structure. Also, a matrix $\mathbf{B}_r$ may be introduced for including viscous damper characteristics that obstructs rotation, mentioned in Section 5.4. An extended equation of motion for a pulley yields

$$\mathbf{M}_r\ddot{\mathbf{d}} + \mathbf{C}_r\dot{\mathbf{d}} + \mathbf{K}_s\mathbf{r}_C + \mathbf{\Phi}_{\mathbf{d}}^T\boldsymbol{\lambda}_r = -\mathbf{Q}_c \tag{7.26}$$

Thus far, the dynamic characteristics of a pulley defined as a rigid body in the Cartesian coordinate system has been defined, yet, the interaction of the cable and pulley remains.

8

Dynamic contact forces and kinematic constraints

Geometrical ideas correspond to more or less exact objects in nature, and these last are undoubtedly the exclusive cause of the genesis of those ideas.

— *Albert Einstein*

A well known challenge within FEA, is modelling contact and friction, its importance and ubiquity has led to extensive attention over the last decades due to its scientific challenge. In order to describe the impact, and contact phenomenons that occur in a cable and pulley system, intelligent algorithms for detecting interaction and its frictional behaviour are essential to obtain a reliable behaviour in simulations.

When establishing a relation between interacting bodies, one need to considerate the most appropriate contact formulation for the task. The contact forces are necessary for obtaining a realistic behaviour that portrays the dynamics of a system, thus, relates to the system dynamics. The necessary forces for constraining its motion are called forces of constraints. Constraints are restrictions that limit the motion of particles and objects in a system, thus, relates to the system kinematics.

Several literature has been reviewed on the matter of describing contact within the field of flexible multibody dynamics. It has been discovered significant progress within this field during the last two decades. This chapter provides a description of how to model the contact between a cable and a pulley properly, based on methodologies from recent works.

8.1   Normal contact force

Friction forces are directly dependent on the normal forces of contact between interacting bodies, is it critical to determine accurate contact forces in order to obtain an accurate representation of friction. In the field of multibody dynamics, this can be a challenge. Contact forces are usually determined by the means of imaginary penetration between objects, or determined by integration of weak form differential equations through the principle of virtual work.

Formulations based on the classical Hertzian model of contact, are often applied in FEM applications due to its simplicity, physical interpretation, and ability for physical verification. Thus, makes it manageable to deal with in numerical formulations, and the foundation of almost all available contact force models [61]. According to the theory, the contact pressure depends on penetration between two contacting surfaces and the geometries of the bodies. However, due to its lack of portraying energy dissipation during impact, the Hertzian contact theory is inadequate for describing these problems by itself [62]. Thus, this model cannot be used for describing the exact behaviour that occurs during the compression and restitution phases of contact. This issue has lead to extensive research, in order for enhancing the Hertzian model to accommodate energy dissipation in the form of internal damping.

Two examples which have been extensively used to model and simulate multibody systems that involve contact, is the formulations proposed by Lankarani & Nikravesh [63], and Hunt & Crossley [64]. However, Machado et al. [61] recently performed a detailed review on the enhanced Hertz formulations. It is emphasised that more recent developments such as Gonthier et al. [65] among others, provide more exact solutions for an impact between objects in the dynamic equations of motion.

Thus, in order to describe a multibody system subjected to impact between two bodies, appropriate contact force models must be adopted. The Gontier et al. normal force model can be written as follows

$$f_n = K\delta^n \left[1 + \frac{1 - c_r^2}{c_r} \frac{\dot{\delta}}{\dot{\delta}^{(-)}} \right] \tag{8.1}$$

in which δ is the relative penetration between the surfaces, $\dot{\delta}$ the relative velocity of penetration, and $\dot{\delta}^{(-)}$ the initial impact velocity. The model degenerates to the original Hertz theory, if the coefficient of restitution $c_r = 1$ which describes perfect elastic contact, and purely inelastic contact if $c_r = 0$ [61]. In order to describe different interaction scenarios, is n a positive exponent that reflects the shape of the contacting surfaces. The contact stiffness K between the contacting surfaces is described by material properties and geometry of the bodies i.e. sphere to sphere, sphere to surface etc.

A challenge is to determine the contact parameters K and n, due to complex geometry of a stranded wire-rope which often consists of single-, double- and multi-helical rope configurations [35]. The contact characteristics between the cable and pulley varies with the configuration of the cable. Figure 8.1a illustrates a single stranded cable, one can assume the interaction areas of contact consists of lines or rectangular shapes, generated between i.e. cylinders. For double- and multi-helical configurations, one may assume circular or ellipsoidal contact areas as figure 8.1b illustrates. For simplicity, the case of a

(a) Single stranded
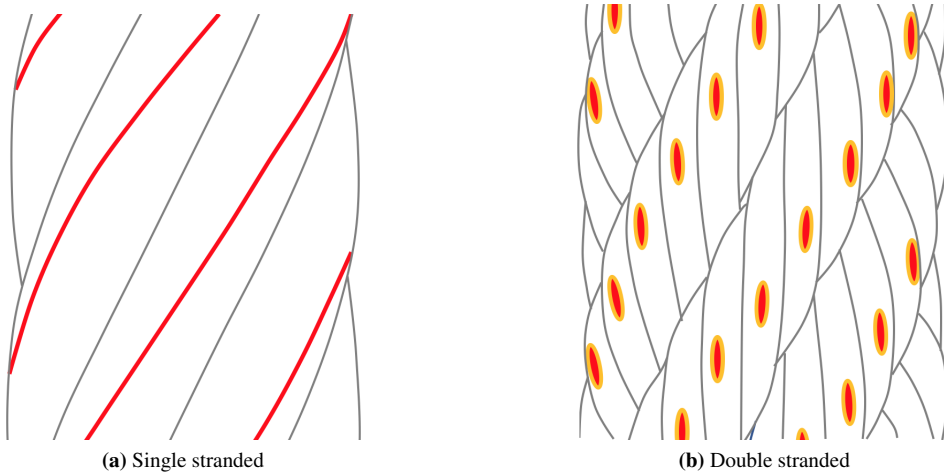
(b) Double stranded

Figure 8.1: Contact areas for single- and double-helical cable configurations.

single stranded wire rope is further discussed. The elliptic case of contact is rather complex in comparison, but fully manageable after referencing literature [35, 66] that has dealt with similar issues.

Cylinder to surface contact

(a) Arc length of interaction

(b) Single-stranded cable in groove
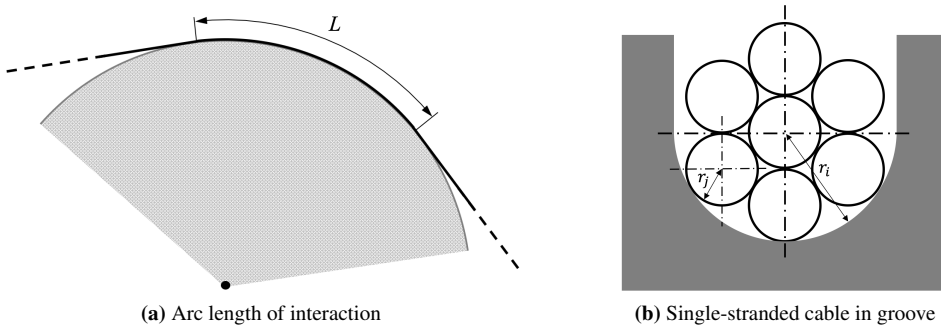
Figure 8.2: Contact domain.

Considering a scenario of single-helical rope configuration, the parameters should be considered cylinder to surface. Unfortunately, the stiffness and geometry parameters are not easily obtained. Pereira et al. [67] suggested the following empirical formulation:

$$K_{cyl} = \frac{(a\Delta r + b)LE*}{\Delta r} \tag{8.2}$$

In this scenario, L denotes the helical arc length of interaction along the pulley, illustrated in figure 8.2a. This relates to the geometrical relation of the stranded rope, and the pulley. The material properties of the contacting surfaces are assumed to be of similar character, thus the composite modulus is expressed as

$$E^* = \frac{E}{2(1 - \nu^2)} \tag{8.3}$$

Here, since the cable rests in the groove of a pulley, the contact is considered internal. Thus $\Delta r = r_i - r_j$, where r_i is the radius of the groove, and r_j the radius of a wire, illustrated in figure 8.2b.

$$\text{For internal contact} \quad \begin{cases} a = 0.965 \\ b = 0.0965 \\ n = Y\Delta r^{-0.005} \end{cases}$$

$$Y = \begin{cases} 1.51[\ln(1000\Delta r)]^{-0.151} & \text{if} \quad \Delta r \in [0.005, 0.34954]\text{mm} \\ 0.0151\Delta r + 1.151 & \text{if} \quad \Delta r \in [0.34954, 10.0]\text{mm} \end{cases}$$

If one studies Y, one can observe its valid range is quite limited. In the real world, a groove can have a much larger radii than the wire i.e. $r_i \gg r_i \rightarrow \Delta r \gg 10mm$. Hunt [64] suggested a value between 1 and 1.5 is adequate for describing cylindrical conditions. Empirical investigations carried out by Brändlein [61, 68] suggests a value of $n = 1.08$ to be adequate for this kind of contact.

8.2 Cable-pulley friction
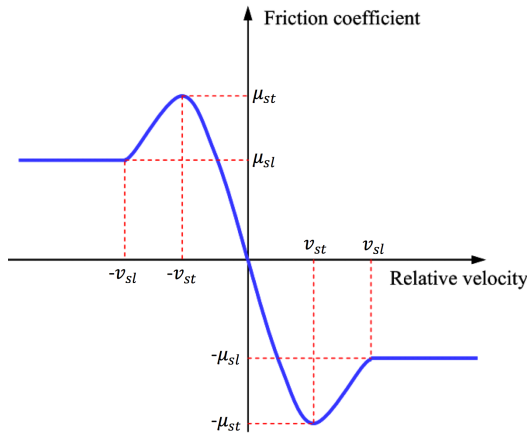
Figure 8.3: Stick slip friction model [69]

An interaction of this kind can be described by different models of friction. The classical ones are typically Coulomb friction, viscous friction and the Stribeck effect [70]. In this

case, the surfaces are considered to be dry, and the Coulomb friction combined with the Stribeck effect are considered. Thus, the states of stick and slip are described by static and dynamic coefficients of friction μ_{st} and μ_{sl} respectively, which directly relates to the normal and tangential forces[65].

If one studies the stick-slip model in figure 8.3 one can notice the friction is a function of the relative velocity between the two surfaces. This raises an issue because it is contrary to considerations discussed in Section 5.4 of preventing sliding between the surfaces.
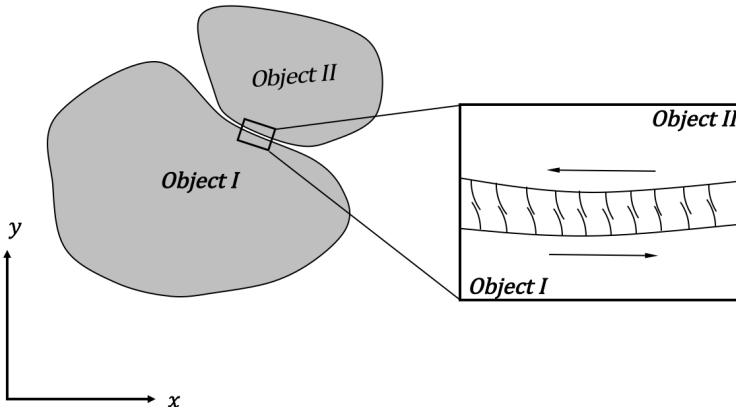
Figure 8.4: Brush bristle friction model

In order to cope with this challenge, the stick-slip model can be considered as a displacement function between the interacting objects [69]. There are several ways of doing so, one of the recurring approaches during this research, is to model the contact as an imaginary brush bristle [12, 65, 71]. As of noted in Section 5.4, a saturation value must be exceeded in order for the surfaces to slide. In the brush bristle approach, the key idea is to define the stiction force by denoting a stiffness-damper function to the bristle, describing the limit of saturation.

$$f_n\mu_{st} = (k_b s + c_b \dot{s}) \tag{8.4}$$

Here, k_b is the bending stiffness of the bristles, c_b denotes the viscous damper coefficient, s and $\dot{s}$ describes relative displacement and velocity, respectively. A saturation value is determined by the static friction at the tip of the bristle, for a given value of the static friction coefficient μ_{st}. The friction force $f_n\mu_{st}$ should never exceed the saturation value $(k_b s + c_b \dot{s})$. The displacement between the contact- and stiction point during sticking, is determined by its elastic displacement $(f_n\mu_{st})/k_b$. Thus, whenever the value of $(k_b s + c_b \dot{s})$ exceeds the saturation value, slip occurs.

8.3 Contact forces and kinematic constraints

A simple, yet clever approach for defining the cable-pulley interaction has been adopted [12, 24, 15] and is a widely used methodology, introducing few variables for describing the contact force. The normal forces acting on an ANCF beam are calculated using the contact model from Section 8.1, which allows penetration. Thus, the contact forces of the system are expressed as follows:
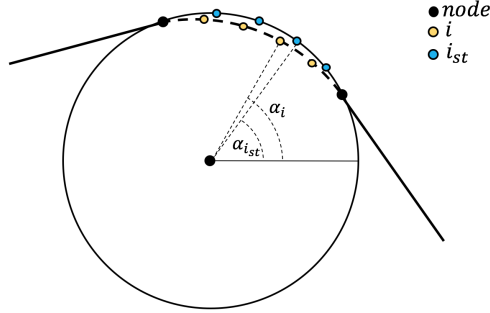
Figure 8.5: Interaction model.

$$\delta = R - \left| \mathbf{r}_i - \mathbf{r}_C \right| \tag{8.5}$$

Here, δ denotes the radial penetration, $\mathbf{r}_C$ the absolute position of the pulley centre, $\mathbf{r}_i$ is the position of a cable-pulley interaction point, and R its radius. Since higher-order beam elements are applied, the contact forces can be distributed along the elements, instead of applying a large amount of elements where the loads are concentrated at the nodes. In order to distribute the contact along the arc-length of the elements, a number of contact points i (integration points) that corresponds with *Gauss-Legendre quadrature*, are introduced on each element. When one of these points coincides with the pulley for the first time, a stiction point i_{st} is introduced to the system. The contact forces are evaluated out from these points in every time step, through Gauss-Legendre integration, obtaining a vector of generalised contact forces. As time integration goes on, these two points might not coincide since the stiction points are rigidly attached to the pulley, whereas the contact point moves along with the cable.

$$s = R(\alpha_i - \alpha_{i,st}) \tag{8.6}$$

The normal vector $\mathbf{n}$, and tangent vector $\mathbf{t}$, on the pulley surface at its contact point i_{st}, is a pair of orthonormal vectors determined by the radial position

$$\mathbf{n} = \frac{\mathbf{r}_i - \mathbf{r}_C}{\left| \mathbf{r}_i - \mathbf{r}_C \right|} \qquad \text{and} \qquad \mathbf{t} = \frac{\mathbf{r}'_i}{\left| \mathbf{r}'_i \right|} \tag{8.7}$$

The normal and tangential velocity of the penetration are described respectively

$$\dot{\delta} = -\dot{\mathbf{r}}_i^T \mathbf{n} \qquad \text{and} \qquad \dot{s} = -\dot{\mathbf{r}}_i^T \mathbf{t} - (R - \delta)\omega \tag{8.8}$$
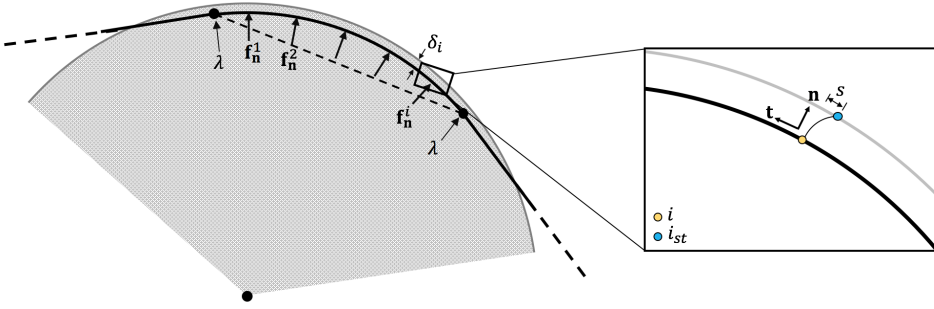
Figure 8.6: Penetration between cable and pulley.

From Section 8.1, the normal contact force are obtained through the model proposed by Gonthier et al. and are expressed in a vector from as follows

$$\mathbf{f}_n^i = K\delta^n \left[1 + \frac{1 - c_r^2}{c_r} \frac{\dot{\delta}}{\dot{\delta}(-)} \right] \mathbf{n}_i \tag{8.9}$$

Stating that a normal contact force can be represented as a nonlinear spring-damper pair, expressed as a nonlinear power function due surface stiffness. Furthermore, the tangential friction force can be modelled with stick-slip characteristics, the stiction force is modelled as the fictitious brush bristle, presented in Section 8.2. The deflection is of the bristle is modelled as a linear spring-damper in the range of lower velocities, expressing the saturation value for the stick-slip limit.

$$\mathbf{f}_{st} = -(k_b s + c_b \dot{s})\mathbf{t} \tag{8.10}$$

where the bending stiffness of the brush bristle is denoted k_b, and c_b the viscous damper coefficient. As emphasised in Section 8.2, the saturation value should never be exceeded. Thus, whenever the value of $(k_b s + c_b \dot{s})$ exceeds the saturation value $f_n \mu_{st}$, slip occurs and the stiction angle between the cable and pulley needs to be updated. The new tangential force and the angle is obtained as follows

$$\mathbf{f}_{st} = -sgn(s)\mu_{st}f_n\mathbf{t} \tag{8.11}$$

$$\alpha_{st} = \alpha - sgn(s)\eta_{st}\frac{\mu_{st}f_n}{k_b R} \tag{8.12}$$

where $sgn(s)$ is a function who returns 1 if $s \geqslant 0$, and returns -1 otherwise. η_{st} represents the amount of bristle deflection in the saturation state, and is a factor for improving the numerical behaviour.

However, if the saturation point is exceeded, and sliding occurs, the tangential force is calculated by means of pure Coulomb sliding friction, using a dynamic friction coefficient μ_{sl}, which is lower than the static friction.

$$\mathbf{f}_{sl} = -sgn(\dot{s})\mu_c f_n\mathbf{t} \tag{8.13}$$

Thus far, the models of stick and slip friction has been established, the expression of the tangential forces can be assembled into a formulation that describes transition between the two friction modes.

$$\mathbf{f}_t \quad \begin{cases} \mathbf{f}_{st} & \dot{s} \leqslant \nu_{st} & \text{sticktion force} \\ \mathbf{f}_{sl} & \dot{s} > \nu_{st} & \text{slipping force} \end{cases}$$

Here, ν_{st} represents the relative velocity between the cable and pulley, whenever it exceeds $\dot{s}$, a transition between the modes of stick- and slip friction occurs. A smoothing function ϑ is introduced for making the transition between stick and slip more numerically friendly.

$$\vartheta = e^{-(\frac{\dot{s}}{\nu_{st}})^2} \tag{8.14}$$

The final expression for the tangential force yields the following formulation

$$\mathbf{f}_t = \vartheta \mathbf{f}_{st} + (1 - \vartheta)\mathbf{f}_{sl} \tag{8.15}$$

The contact forces distributed over the arc-length of contact in any given element is summarised into the following vector

$$\mathbf{f}_{c,i} = \mathbf{f}_n^i + \mathbf{f}_t^i \tag{8.16}$$

Which describes the generalised contact forces as the sum of the interaction forces of each point i in an element subjected to contact. As means to define the generalised forces distributed over the contacting arc-length, *Gauss-Legendre quadrature* is applied instead of symbolic evaluation of the integral, since the symbolic integration of this integral would require the forces to be expressed as a function of the material coordinate ξ. Instead, it is evaluated in certain points along the interacting arc.

$$\mathbf{Q}_c = l \int_0^l \mathbf{f}_c(x)^T \mathbf{S}(x)^T dx = l \int_0^1 \mathbf{f}_c(\xi_i)^T \mathbf{S}(\xi_i)^T d\xi \tag{8.17}$$

$$\approx \frac{l}{2} \sum_{i=1}^k w_i \mathbf{f}_{c,i}(\xi_i)^T \mathbf{S}(\xi_i)^T, \qquad \xi_i = \frac{x_i + 1}{2}, \quad i = 1, 2, 3..., k.$$

This is an approximate value instead of an exact integration. $\mathbf{S}$ denotes the global shape function matrix in given in equation 7.3, ξ_i is the integration points along the arc-length, described by x_i in the global frame, and w_i Gaussian weight numbers. The penetration in the contact points is defined by the position of the cable, when points of the cable penetrate the pulley, the normal contact force will arise. The matrix $\mathbf{Q}_c$ accounts for the contact forces, and are included in the matrix of generalised external forces, $\mathbf{Q}(\mathbf{e}, \dot{\mathbf{e}}, t)$. An advantage of using the ANCF in this kind of contact formulation, is that it is easy to detect interaction before the calculation procedure of contact. In the global positions of the cable that is not nearby a pulley, there is no reason for checking the forces in the integration points of that domain, neither any need to determine the limits of the contacting area, since the forces are checked when evaluating the integral in equation 8.17.
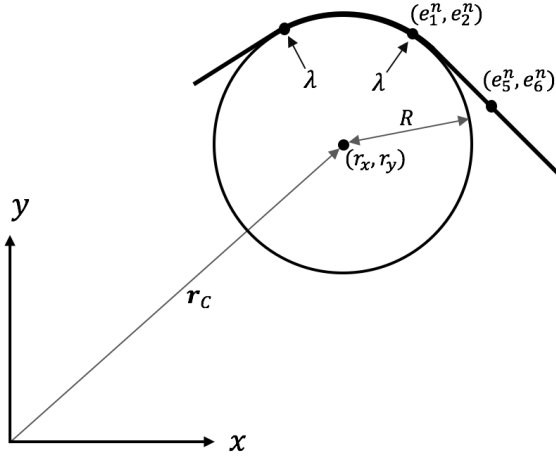
Figure 8.7: Illustration of constraint forces.

Hitherto, only the contact forces of the cable interacting with the pulley has been established, this is not enough for modelling the behaviour of a complete system of cable and pulleys.

Kinematic constraints has to be introduced for obtaining a complete simulation. The absolute position of a node at on an ANCF element, n, can be kinematic constrained with respect to the contact penetration, as follows

$$\mathbf{\Phi}(\mathbf{e}, t) = \begin{cases} \Phi_1 & = (e_1^n(t) - r_x)^2 + (e_2^n(t) - r_y)^2 - (R - \delta)^2 \geqslant 0 \\ \Phi_2 & = (e_5^n(t) - r_x)^2 + (e_6^n(t) - r_y)^2 - (R - \delta)^2 \geqslant 0 \\ . \\ . \\ . \\ \Phi_r \end{cases}$$

Summarising this constraint for all nodes yields the constraint matrix $\mathbf{\Phi}$, containing all the constrained relation of the cable with respect to a pulley.

Due to this contribution of representing contact forces and kinematic constraints, there is no need for an unnecessarily large amount of elements for obtaining a realistic behaviour [15]. In other words, by the introduction of contact points, one reduces the required amount of elements in a conventional approach for obtaining an equally adequate representation of contact forces.

Since the cable and pulley are already defined in a global Cartesian coordinate system, it can be combined with other rigid and flexible bodies also defined in this system [56].

8.4   Rigid-flexible multibody systems

Thus far, only the cable and its interaction with a pulley has been described, the two dimensional system may contain an arbitrary set of N_r rigid- and N_f flexible bodies, assembled by different sorts of joints. Both the flexible- and rigid bodies are defined in the global frame, and leads to a mixed formulation in which all system coordinates are defined with respect to the global coordinate system. If one assumes these bodies to be interconnected through rigid-, revolute- or sliding joints, the system should be treated as a single body [51]. A vector that collects all the coordinates of the system yields

$$\mathbf{p} = \begin{bmatrix} \mathbf{d}^T & \mathbf{e}^T \end{bmatrix}^T \tag{8.18}$$

Here, $\mathbf{e}$ represents the nodal coordinates of all flexible bodies in the system, while $\mathbf{d}$ contains all the rigid body coordinates. If one assumes these bodies to be interconnected through linear kinematic constraints, one can reduce the sets of coordinates.

$$\mathbf{d} = \begin{bmatrix} \mathbf{d}^T & \cdots & \mathbf{d}_k^T & \cdots & \mathbf{d}_{N_r}^T \end{bmatrix}^T, \quad \mathbf{e} = \begin{bmatrix} \mathbf{e}^T & \cdots & \mathbf{e}_k^T & \cdots & \mathbf{e}_{N_f}^T \end{bmatrix}^T \tag{8.19}$$

The vector for the reduced nodal coordinates of the flexible body with linear kinematic constraints are given as

$$\mathbf{e} = \mathbf{T}_f \tilde{\mathbf{e}} \tag{8.20}$$

Where $\tilde{\mathbf{e}}$ is a new vector of nodal coordinates And the linear kinematic constraints between rigid and flexible bodies is given as follows

$$\tilde{\mathbf{e}} = \begin{bmatrix} \mathbf{T}_{rf} & \mathbf{T}_{ff} \end{bmatrix} \begin{bmatrix} \mathbf{d} \\ \hat{\mathbf{e}} \end{bmatrix} \tag{8.21}$$

The vector of rigid body coordinates is reduced as following

$$\mathbf{d} = \mathbf{T}_r \hat{\mathbf{d}} \tag{8.22}$$

The final vector containing all the reduced coordinates of the system has the expression

$$\mathbf{q} = \begin{bmatrix} \hat{\mathbf{d}}^T & \hat{\mathbf{e}}^T \end{bmatrix}^T \tag{8.23}$$

Where $\hat{\mathbf{d}}$ and $\hat{\mathbf{e}}$ are the new reduced vectors of rigid and flexible nodal coordinates respectively. Using this method of coordinate reduction, the final vector relation of the system yields

$$\mathbf{p} = \mathbf{T}\mathbf{q} \tag{8.24}$$

where $\mathbf{T}$ are a transformation matrix between the rigid and flexible bodies of the system, and $\mathbf{q}$ yields the new reduced vector of system coordinates.

$$\mathbf{T} = \begin{bmatrix} \mathbf{T}_r & \mathbf{0} \\ \mathbf{T}_f \mathbf{T}_{rf} \mathbf{T}_r & \mathbf{T}_r \mathbf{T}_{ff} \end{bmatrix} \tag{8.25}$$

A full description and derivation of this matrix is performed in the literature of García-Vallejo et al. [51], where the methodology is explained in detail.

Chapter 9

Dynamic simulation and stabilisation techniques

> Geometry is founded on mechanical practice and is nothing other than that part of universal mechanics which reduces the art of measuring to exact propositions and demonstrations.
>
> *— Sir Isaac Newton*

The reaction forces and the constraints has been defined for the cable and pulley, and methods for assembling the model into a more complex system was discussed, the methods for solving the system is however another challenge.

Dealing with multibody systems involves two phases, the first is development of mathematical models of the system, secondly, implementation of computational procedures to perform the simulation, analysis and optimisation of the global motion.

9.1 Constraints and solver methods

Simulating this kind of problem can be challenging due to sudden surges in acceleration values during the time evolution of the system [53]. Considering a multibody system based the presented formulations, the most commonly used method for formulating the motion equations for more complex constrained multibody systems, applies *Lagrange's equations*, expressed as follows [72, 73]

$$\frac{d}{dt}\left(\frac{\partial E_k}{\partial \dot{\mathbf{q}}}\right) - \frac{\partial E_k}{\partial \mathbf{q}} = \mathbf{Q_q} - \frac{\partial E_p}{\partial \mathbf{q}} - \frac{\partial R}{\partial \dot{\mathbf{q}}} + \mathbf{\Phi^T}\boldsymbol{\lambda} \tag{9.1}$$

where R denotes the *Raylegh's dissipation* function, the rest of the terms are presented through Chapter 7 and 8. In dynamic multibody systems, the constraints are often dependent on the relations between the position variables, these are referred to as holonomic constraints. If the time variable appears explicitly in the relations of the constraint, it is referred to as rheonomic constraints. These constraint formulations enables the description of motion without paying any explicit attention to the forces of constraint. For a constrained multibody system, the contact can be described typically by a set of nonlinear holonomic rheonomous algebraic equations

$$\mathbf{\Phi}(\mathbf{q}, t) = \begin{bmatrix} \mathbf{\Phi}(\mathbf{d}, t) \\ \mathbf{\Phi}(\mathbf{e}, t) \end{bmatrix} = \mathbf{0} \tag{9.2}$$

which assembles all the constraints of the system. This term needs to be differentiated into a Jacobian matrix in order to apply the constraint to the equation of motion [73].

$$\begin{aligned} \mathbf{\Phi_q} = \left(\frac{\partial \mathbf{\Phi}}{\partial \mathbf{q}}\right) = \left[\frac{\partial \Phi_r}{\partial q_j}\right] \\ r = 1, 2, 3, ..., p, \\ j = 1, 2, 3, ..., n, \end{aligned} \tag{9.3}$$

Here, r denotes the number of constraints equations (geometric and kinematic), and j represents a set of unknown depended generalised coordinates. The number of dynamic degrees of freedom in the system becomes $f = j - r$ [60]. Differentiating equation 9.2 with respect to time yields the velocity constraint equations, after double differentiating the constraint matrix with respect to time, vector $\boldsymbol{\gamma}(\mathbf{q}, \dot{\mathbf{q}}, t)$ contains the remaining terms of the differentiated constraints, and the acceleration constraints are obtained as follows

$$\mathbf{\Phi_q}\ddot{\mathbf{q}} = \boldsymbol{\gamma}(\mathbf{q}, \dot{\mathbf{q}}, t) \tag{9.4}$$

There are several methods available for enforcing the contact constraints, the most prominent ones for solving contact is known as the penalty method, the Lagrange multiplier method, and the augmented Lagrange method [74], which are normally applied in computational problems like these [75, 53]. The mentioned methods have all pros and cons, and in order to choose one most suitable for the task, they have to be discussed for its purpose. It is therefore intended for discussion of possible methods for the solution of motion in multibody systems.

9.1.1 The Penalty Method

The penalty method has been widely used to model contact forces due to its straightforward computer implementation, there are no introduction to additional equations and the method is easy to understand from a physical point of view. The physical interpretation of the penalty method is to consider a very stiff spring between nodes involved in the prescribed constraint, this is referred to as a penalty element, and its stiffness a penalty weight α. However, this method only satisfy the constraint conditions approximately, when introducing a finite penalty weight to an arbitrary constraint between two nodes e.g. $u_1 = u_2$, a gap error occurs $\left|e_g\right| = u_1 - u_2$, that violates the constraint. In order for reducing the violation, $e_g \rightarrow 0$, one may increase the weight number $\alpha \rightarrow \infty$, however, this procures an ill-conditioned stiffness matrix due to inversion. In other words, we obtain two effects that odds with each other. As means for obtaining convergence to an exact solution by increasing the weight number, one inflicts numerical instability and the solution error is increased [20, 49, 76]. Yet, this method is efficient for describing problems concerning friction contact as a result of the penetration, i.e. gap error. Introducing the constraint equations to the system by terms of the penalty method, the equation of motion is expressed as follows:

$$\mathbf{M_q \ddot{q}} + \mathbf{\Phi}_q^T \alpha \mathbf{\Phi} = \mathbf{Q}(\mathbf{q}, \dot{\mathbf{q}}, t) \tag{9.5}$$

However, this method is automatically disqualified in order for obtaining the constant distance constraints that defines the pulley as rigid, due to the gap error.

9.1.2 The Lagrange multiplier method

Lagrange multipliers has long been used in mathematical optimisation techniques as a strategy for finding the maxima and minima of functions subjected to constraints, e.g. if a function $f(x, y)$ is constrained by another function $g(x, y)$, one can determine its maxima and minima when the criterion of parallel gradients is fulfilled

$$\nabla f = \lambda \nabla g \tag{9.6}$$

A physical interpretation of the Lagrange multiplier is to consider it as a reaction force, i.e. a constraint force imposing displacement restrictions [49, 76]. The Lagrange multiplier has proven to work as an efficient variable for enforcing the constraint conditions, instead of enforcing the system with very large penalty weights, introduces a set of Lagrange multipliers at each constraint which represents a reaction force, however the multipliers are unknowns, leading the method to suffer from so-called *drift-off* problems, violating the constraint conditions. Dealing with this problem one need to introduce additional stabilisation techniques for avoiding unwanted motions in the system [73].

$$\mathbf{M\ddot{q}} - \mathbf{\Phi_q^T \lambda} = \mathbf{Q}(\mathbf{q}, \dot{\mathbf{q}}, t) \tag{9.7}$$

The Lagrange multipliers relates to the constraint conditions $\mathbf{\Phi} = 0$, and acts in the direction of the constraint, illustrated by figure 8.7. Also, the multipliers do not alter the energy of a system.

9.1.3 Augmented Lagrangian method

Along with the most conventional techniques discussed above, the augmented Lagrangian method is often chosen to cope with the contact equality constraints [76]. The method was first introduced by Hestenes [77] and has afterwards been diversely used in fields dealing with mathematical optimisation of some sort. What this method practically do, is to combine the penalty- and Lagrange method. The contact is determined by an augmented procedure for enforcing the constraints, first, it determines the contact forces from the gap error and the penalty weight, i.e. as a spring force. When the contact forces is revealed, the magnitude of the Lagrange multipliers are determined, correcting the "gap error" and the solution becomes exact. By applying this method, the equations of motion for the whole multibody system has the form [78]

$$\mathbf{M}\ddot{\mathbf{q}} + \mathbf{\Phi_q^T}\alpha\mathbf{\Phi} + \mathbf{\Phi_q^T}\boldsymbol{\lambda}^* = \mathbf{Q}(\mathbf{q}, \dot{\mathbf{q}}, t) \tag{9.8}$$

where the multipliers are obtained by the following iteration process given by sub-index k

$$\boldsymbol{\lambda}_{k+1}^* = \boldsymbol{\lambda}_k^* + \alpha\mathbf{\Phi}_{k+1} \tag{9.9}$$

This method is known to be the most numerically stable one, which combines the best from two worlds, and maybe the most successful method for simulating problems of contact. However, its iteration process is significantly larger in comparison, as illustrated by its equations.

9.2 Dynamic simulation and stabilisation techniques

For this purpose, the Lagrange multiplier method is chosen to cope with the constrained multibody system. The method is able to handle complex constraint equations, e.g slave nodes can depend on other slaves as well as masters [49]. However, the method increases the number of unknowns, but in contrast to the penalty method, the Lagrange multiplier method has the advantage of being exact. As of noted, it is not as numerically stable as the augmented Lagrangian method, yet, more computationally cost efficient.

Introducing a vector of Lagrange multipliers $\boldsymbol{\lambda}$ to the particular expression, containing a multiplier for each constraint. Substituting it into the generalised forces of motion, and equation 9.7 is obtained.

Assembling the motions of the systems from equation 7.18 and 7.26, along with the contact forces obtained form 8.17 and the constraints 9.2, yields the complete system of equations. This is often referred to as a *monolithic system*, which fully describe the cable and pulley as a system of flexible and rigid bodies

$$\begin{bmatrix} \mathbf{M}_f & \mathbf{0} & \mathbf{\Phi_e}^T \\ \mathbf{0} & \mathbf{M}_r & \mathbf{\Phi_d} \\ \mathbf{\Phi_e} & \mathbf{\Phi_d} & \mathbf{0} \end{bmatrix} \begin{bmatrix} \ddot{\mathbf{e}} \\ \ddot{\mathbf{d}} \\ -\boldsymbol{\lambda} \end{bmatrix} = \begin{bmatrix} \mathbf{Q}(\mathbf{e}, \dot{\mathbf{e}}, t) \\ \mathbf{Q}(\mathbf{d}, \dot{\mathbf{d}}, t) \\ \boldsymbol{\gamma}(\mathbf{q}, \dot{\mathbf{q}}, t) \end{bmatrix} = \begin{bmatrix} \mathbf{Q_e} + \mathbf{Q_c} - \mathbf{B}_f\dot{\mathbf{e}} - \mathbf{Ke} \\ -\mathbf{Q}_c - \mathbf{B}_r\dot{\mathbf{d}} - \mathbf{K}_s\mathbf{r}_C \\ \boldsymbol{\gamma}(\mathbf{q}, \dot{\mathbf{q}}, t) \end{bmatrix} \tag{9.10}$$

Written in a compact form

$$\begin{bmatrix} \mathbf{M} & \mathbf{\Phi_q}^T \\ \mathbf{\Phi_q} & \mathbf{0} \end{bmatrix} \begin{bmatrix} \ddot{\mathbf{q}} \\ -\boldsymbol{\lambda} \end{bmatrix} = \begin{bmatrix} \mathbf{Q}(\mathbf{q}, \dot{\mathbf{q}}, t) \\ \boldsymbol{\gamma}(\mathbf{q}, \dot{\mathbf{q}}, t) \end{bmatrix} \tag{9.11}$$

The presented equation model is an effective way of solving for the motion in a system, containing good representation of the kinematic constraints. However, this method does not explicitly use the constraint equations for position and velocity, allowing for a drift in the system constraints due to numerical approximations, round-off errors etc. These are often referred to as drift-off effects. In order to deal with this issue, the well known *Baumgarte stabilisation technique* can be applied to keep the constraint violation during numerical time integration under control [73, 61]. Thus, the constraint equations can be modified as follows

$$\ddot{\mathbf{\Phi}} + 2\alpha \dot{\mathbf{\Phi}} + \beta^2 \mathbf{\Phi} = 0 \tag{9.12}$$

Which yields a modified vector of the acceleration constraints.

$$\bar{\boldsymbol{\gamma}}(\mathbf{q}, \dot{\mathbf{q}}, t) = \boldsymbol{\gamma}(\mathbf{q}, \dot{\mathbf{q}}, t) - 2\alpha \dot{\mathbf{\Phi}} - \beta^2 \mathbf{\Phi} \tag{9.13}$$

Thus, a stabilised version of equation 9.4, and the new accelerations of the system are obtained from

$$\mathbf{\Phi_q} \ddot{\mathbf{q}} = \bar{\boldsymbol{\gamma}}(\mathbf{q}, \dot{\mathbf{q}}, t) \tag{9.14}$$

Here, α and β are positive constants representing feedback control parameters for the velocities and constraint violations. A disadvantage with this procedure is that any general method for decent selection of these, does not exist. More details how to determine α and β are discussed by Hajžman et al. [73].

$$\begin{bmatrix} \mathbf{M} & \mathbf{\Phi_q}^T \\ \mathbf{\Phi_q} & \mathbf{0} \end{bmatrix} \begin{bmatrix} \ddot{\mathbf{q}} \\ -\boldsymbol{\lambda} \end{bmatrix} = \begin{bmatrix} \mathbf{Q}(\mathbf{q}, \dot{\mathbf{q}}, t) \\ \bar{\boldsymbol{\gamma}}(\mathbf{q}, \dot{\mathbf{q}}, t) \end{bmatrix} \tag{9.15}$$

In order to solve the system numerically, equation 9.7 is rearranged for describing the motion

$$\ddot{\mathbf{q}} = \mathbf{M}^{-1}(\mathbf{Q} + \mathbf{\Phi_q^T} \boldsymbol{\lambda}) \tag{9.16}$$

substituting equation 9.16 into 9.14, followed by rearranging yields

$$\bar{\boldsymbol{\gamma}}(\mathbf{q}, \dot{\mathbf{q}}, \mathbf{t}) = \mathbf{\Phi_q} \mathbf{M}^{-1}(\mathbf{Q} + \mathbf{\Phi_q^T} \boldsymbol{\lambda}) \tag{9.17}$$

$$\boldsymbol{\lambda} = (\mathbf{\Phi_q} \mathbf{M}^- \mathbf{\Phi_q^T})^{-1}(\bar{\boldsymbol{\gamma}} - \mathbf{\Phi_q} \mathbf{M}^{-1} \mathbf{Q}) \tag{9.18}$$

Substituting equation 9.18 into 9.16, vector $\boldsymbol{\lambda}$ can be eliminated, and thus, the final equation of motion for the system yields

$$\ddot{\mathbf{q}} = \mathbf{M}^{-1} \mathbf{\Phi_q^T} (\mathbf{\Phi_q} \mathbf{M}^{-1} \mathbf{\Phi_q^T})^{-1}(\bar{\boldsymbol{\gamma}} - \mathbf{\Phi_q} \mathbf{M}^{-1} \mathbf{Q}) + \mathbf{M}^{-1} \mathbf{Q} \tag{9.19}$$

9.3 Considering real-time simulation

The simulation of a digital twin, that is happening in in real-time, requires an analysis time smaller than the physical time used by the actual motion of the physical system. In other words, the computational time needs to be smaller than the time step selected. Thus, choosing a suitable method used for the integration of motion is critical. It is therefore required that the time integrator performs well during the simulation.

Explicit multistep methods is known to be inexpensive and accurate if small enough time steps are chosen, however it do not provide sufficient stability conditions. The methods chosen for real time simulation should therefore be implicit, simple step, with good stability properties, sufficiently accurate and computational efficient in terms of CPU power required. It is therefore convenient to apply implicit single step integration formula with fixed time steps and order, requiring the same computational cost of each integration step and capable at adjusting to system discontinuities.

According to these requirements the Newmark β-integration [79] family is a suitable choice [60]. Further, the WTZ-α method [80], HHT-α method [81] and implicit Runge-Kutta method [82] are all suitable choices for time integration of the equations of motion [60, 83]. However, the WTZ- and HHT-α method seems to be more preferable than the more computational expensive implicit Runge-Kutta method [60]. Newmark β−integration with HHT-α stability has already been demonstrated in digital twin applications carried out by SAP Fedem [7], thus a natural choice. If equation 9.19 is to be solved by the Newmark β−integration which was originally obtained from the Taylor series expansion about time, the numerical time integration is carried out as follows [8]:

$$\dot{\mathbf{q}}_{k+1} = \dot{\mathbf{q}}_k + (1-\gamma)\Delta t \ddot{\mathbf{q}}_k + \gamma \Delta t \ddot{\mathbf{q}}_{k+1} \tag{9.20}$$

$$\mathbf{q}_{k+1} = \mathbf{q}_k + \Delta t \dot{\mathbf{q}}_k + \left(\frac{1}{2}-\beta\right)\Delta t^2 \ddot{\mathbf{q}}_k + \beta \Delta t^2 \ddot{\mathbf{q}}_{k+1} \tag{9.21}$$

Here, the sub-index k denotes the increment, and Δt the chosen time step, β and γ are integration parameters, acting as numerical dampers to preserve numerical stability during the simulation. The commonly used values of the Newmark method is ($\gamma \geqslant 0.5$) and ($\beta \geqslant 0.25(\gamma + 0.5)^2$) and provides unconditional stability [8].

Yet, it results in numerical oscillations (e.g. observed in fig. 5.8a), the phenomenon is a result of "overshooting" of displacements obtained from the time integration, resulting in residual oscillations, i.e. numerical oscillations. By introducing numerical dissipation, these spurious oscillations are damped on the expense of second order accuracy, and are too disruptive in the lower-frequency domain. Further, the HHT-α and WBZ-α achieves damping for high frequencies, without affecting lower modes and loosing second order accuracy [84]. Also, introducing high frequency dissipation is found to improve the convergence during iteration solving of highly nonlinear problems [85].

However, a method that has shown to have even better dissipation characteristics, which is an enhancement of the Newmark-algorithm that combines the HHT-α and WBZ-α method. Its main advantage is that the method enables for user-controlled high frequency dissipation level, while minimising its impact on the low frequencies. The method is referred to as the Generalized-α method [85] in the literature. This method has identical

displacement and velocity updates as the Newmark algorithm. Yet, with a force balance equation (9.15) containing modified displacement unknowns, expressed as follows

$$\mathbf{q}_{k+1-\alpha_f} = (1 - \alpha_f)\dot{\mathbf{q}}_{k+1} + \alpha_f\dot{\mathbf{q}}_k \qquad (9.22)$$

$$\dot{\mathbf{q}}_{k+1-\alpha_f} = (1 - \alpha_f)\dot{\mathbf{q}}_{k+1} + \alpha_f\dot{\mathbf{q}}_k \qquad (9.23)$$

$$\ddot{\mathbf{q}}_{k+1-\alpha_m} = (1 - \alpha_m)\ddot{\mathbf{q}}_{k+1} + \alpha_m\ddot{\mathbf{q}} \qquad (9.24)$$

and modified time incrimination

$$t_{k+1-\alpha_f} = (1 - \alpha_f)t_{k+1} + \alpha_f t_k \qquad (9.25)$$

According to this formulation, the Generalized-α degenerates to HHT-α if $\alpha_m = 0$, and WBZ-α if $\alpha_f = 0$. Furthermore, if $\alpha_m, \alpha_f = 0$ one obtains the original Newmark formulation. Thus, the Generalized-α is a combination of these three. The algorithm is critically controlled by these parameters, which are determined from the value of its spectral radius at infinity ρ_∞, that is, a user specified value. Thus, one can determine the dissipation parameters, providing an optimal relation between the ρ_∞- dependent dissipation parameters. The spectral radius at infinity may be varied between a value of zero and one, in the case of $\rho_\infty = 1$ there are no dissipation, the smaller the spectral radius, the greater numerical dissipation. The dissipation parameters are obtained as follows

$$\alpha_m = \frac{2\rho_\infty - 1}{\rho_\infty + 1} \quad \text{and} \quad \alpha_f = \frac{\rho_\infty}{\rho_\infty + 1} \qquad (9.26)$$

Where the following relations needs to fulfill the following criteria for absolute stability

$$\alpha_m \leqslant \alpha_f \leqslant \frac{1}{2}, \qquad \beta \geqslant \frac{1}{4} + \frac{1}{2}(\alpha_f - \alpha_m), \qquad \gamma = \frac{1}{2} - \alpha_m + \alpha_f \qquad (9.27)$$

The Generalized-α time integration algorithm is unconditionally stable, second order accurate, and possesses an optimal combination of high- and low frequency dissipation [85]. By applying the Generalized-α, one enables for controlling the high frequency dissipation, and CPU cost. Thus, this algorithm is recommended by the author.

9.4   Brief synopsis of dynamic simulation

According to the method presented, the dynamic responses involves evaluation of vector $\mathbf{Q}$ and $\bar{\boldsymbol{\gamma}}$ for each time step, solving for $\ddot{\mathbf{q}}$. Integrating and double integrating $\ddot{\mathbf{q}}$ with respect to time, and one obtains the velocity $\dot{\mathbf{q}}$ and position vector $\mathbf{q}$ at the given time step respectively. Furthermore, accelerations are together with the velocities time integrated in order to obtain the new velocities and positions for the next time step, which is repeated until the complete motion of the system is solved.

Chapter 10

Closure

Science is about knowing, engineering is about doing

— *Henry Petroski*

10.1   Summary and discussion

The content of this thesis has proven the topic regarding inherent dynamics of cable and pulleys to be a large and complex field of study. An overview in Chapter 4 of the latest researches was presented that relates to, or directly approaches systems that consist of cable and pulleys for simulation tasks. As presented through Chapters 4 and 6, investigating state of the art FE-based modelling of cable and pulleys, revealed that there are several approaches for modelling these kind of systems. There is no right or wrong formulation, and one has to consider the element formulations for its purpose. It was discovered through this research that modelling and simulations of such systems do not have any best practice. Thus, different methods are applied for different investigation purposes.

The basis for the model suggested in this work, has been focused on including physical effects that were presented in Chapter 5. The gathered material for the development is based on physical verified theory obtained from experiments, and has been assembled into a mathematical model.

However, it might be applicable to apply more conventional elements for simulations that involves large and complex constructions, where the dynamics of cable-pulley systems are not of direct interest, but rather, its impact on a structure as a whole. For this task, elements such as the slipring connector [40], the super element approach [13, 14], or even denoting massless springs [9, 11] are considered as reasonable and efficient approaches.

Yet, through the objectives of this work, it was concluded that the ANCF element proved to be the most suitable candidate for describing behaviour of cables, despite its suffering of Possion- and shear locking. The author determined these problems to be negligible due to its occurrence particularly in cases where the element properties is to be considered stiff, but has addressed other more recent ANCF-based formulations that handles these issues.

Thus, it has to be emphasised that modified versions of the ANCF should be taken into consideration, since some of them are recognised as strong candidates to the original element. In cases involving high velocities, an element that includes centrifugal and Coriolis forces [50] should be considered. Also, elements [16, 51, 52] that are potentially more computational efficient needs to be reconsidered for the purpose. In addition, these elements enables for surface distribution of contact forces, which is not obtained in a beam-element, since it is only represented by its centerline. They also introduces additional degrees of freedom that might be important in future studies of spatial dynamic phenomenons.

All the ANCF formulations are based on the *Euler-Bernoulli beam theory*. This theory is based on the assumption of that any cross section of a beam, must remain plain to its centerline. This assumption are valid, but not accurate during large deformation problems. Thus, another importance is to consider formulations based on the *Timoshenko beam theory*. This family of elements are capable of portraying more accurate deformations due to shear in the beam.

However, in the author's opinion, the discussed model is capable of capturing complex dynamic effects, and provides a strong foundation for further investigations that are going to be carried out at SFI. It has been demonstrated that the ANCF formulation is able to handle complex motions [12, 20, 21, 24, 86] that conform with physical experiments [24], requiring low CPU cost enabling for real-time simulations [23].

Yet, researchers who have applied the ANCF-formulation has included physical characteristics of cables by guessing and approximation, which might be a source of error. Thus, the author has suggested more accurate methods for obtaining realistic parameters for the derivation of an element. This is a rather complex task to perform but, is proven to be possible [29, 27, 30], if the configuration of a cable is known. By the knowledge of the author, this has not yet been applied when deriving cable elements for multibody dynamic problems. Based on these works, the mathematical models could be programmed working as a "black-box" for describing the characteristics of bending stiffness, maybe as a variable of a cable curvature. Further, to be included as modified parameters for the derivation of stiffness and damper properties of a cable.

Due to the highly flexible nature of cables, modelling of pulleys as rigid bodies is found to be a reasonable simplification, which also reduces the computational time consume drastically. A rigid body formulation where the physical effects such as inertial- and damper effects included, are suggested. Also, in contrast to other works where pulleys are considered fixed to a point. It is worth emphasising the possibility of denoting movement, elastic properties, and eigenvalues to the pulley fixations, obtained from analyses of a support structure. These properties is conceivable to tabulate or parameterise, dependent on positions of the supporting structure that alters these characteristics.

The interaction forces between the contacting bodies has been suggested to be modelled by means of penetration, based on the Hertz theory. As of noted, this method is inadequate due to its inconsistency of energy dissipation. Other authors [15, 12, 24] which have been dealing with similar problems, have applied the Hunt-Crossley model for describing normal contact. However, through this work it was discovered that other models for normal contact proved to be more exact in comparison with experimental results [61]. Thus, the author suggested a more adequate model for describing the normal contact forces that was first proposed by Gonthier et al. [65] but emphasises the existence of other equivalent force models, that are compared in the literature of Machado et al [61].

Realistic models of contact are essential for obtaining an accurate representation of the frictional characteristics. The tribology of the system is also a very challenging field of study which demands extensive attention in the further work. Thus, the proposed model of contact and friction has been chosen such one easily can substitute these formulations with other more suitable ones to the model. Thermal effects can easily be included, enabling for thermal dependent friction coefficients, also, phenomenons such as friction induced vibrations might be included to the model of friction. If the friction model proves to conform with future physical experiments, the saturation value that describes the sticking limit could for instance work as a stabilisation parameter in a control system, regulating velocities in order to prevent slip.

The chosen method for solving the constrained system, was the conventional Lagrange multiplier method, which is an uncertainty. It was chosen as a mean between the penalty- and the augmented Lagrange method. In the authors opinion, this method seems to be the most suitable one when considering the challenges of computational costs, potentially for the application to a digital twin. It does not require any "black-box" input of constants as the penalty method does, but introduces more equations to the system, yet has the advantage of being exact. Introducing stabilisation techniques for handling drift-offs in the Lagrange multiplier method dealing with the numerical stability provides an exact

solution with less iterations, combined with the Generalized-α algorithm is considered suitable for this purpose.

However, the augmented Lagrange method might be about equally as effective as the conventional Lagrange method, computational wise. Indeed, it has more iterations, but these are to be considered as "iterations within the iterations". Due to the numerical stability which this method provides, one avoids stabilisation techniques required in the conventional Lagrange method. Thus, this is an uncertainty that needs to be reconsidered by following researchers of this topic.

An obvious limitation this model suffers, is its two-dimensional formulation. One needs to verify the integrity of this model in order for further developing it to a three-dimensional model. If this is achieved, implementation in a software such as FEDEM are possible. The literature of Konyukhov and Schweizerhof [87] provides detailed descriptions of mathematical methods of how to prescribe contact of three-dimensional ANCF elements to rigid (or flexible) surfaces.

As a closure to the discussion, the author would like to address other ongoing research related to this topic. The author has been in contact with Bulín et al. at the University of West Bohemia who is very enthusiastic about this study. Their research is motivated on an successfully implementation of the absolute nodal coordinate formulation, together with contact modelling, the research is also motivated by the investigation of dynamics of parallel cable manipulators with active structures.

10.2 Conclusion

The ANCF finite elements are designed for large deformations in multibody dynamic problems. In contradiction to other more conventional systems, the proposed model include all components of the system. The dynamic effects are mathematically described explicit, thus, the proposed model is considered the most prominent for it to function as a mathematical foundation. The formulation has the deliberate intent, constructed such that one easily can manipulate and extend it. In this model, other beam elements can be used, different models of contact, other models for friction, functions describing thermal effects can be included enabling for thermal dependent friction etc.

In the author's opinion, the formulation of cable and pulley through the approach of rigid-flexible multibody dynamics has potential of reaching a high degree of maturity, if relationships between different formulations of objects and their interactions are established. Defining coordinate transformations that relates various formulations as discussed in Section 8.4. Thus, it is believed that the absolute nodal coordinate formulation can effectively be used to achieve the important goal of adequate simulations of cable and pulley systems.

Some of the phenomena that occur at a small scale, influences an entire system that involves contact, friction and inter-layer sliding of wires in a cable has been discussed. Despite its long and profitable history, multibody systems of such character is still an active and challenging research domain. As stated by Schiehlen [88], *"more work is required to better understand the micromechanical phenomena influencing the macro mechanical multibody motion with contact"* .

By utilising the ever-expanding computing power, this model can be implemented in

software for helping engineers solve increasingly complex challenges related to cable and pulleys, band-drives etc. The model might be implemented in a script that includes a post-processor of sensor data instead of fictive loads as in conventional FE-programs. Further to be used in e.g. control systems for offshore cranes, draw works etc. as a stabilisation algorithm for improved performance.

10.3 Further work - research proposals

We can only see a short distance ahead, but we can see plenty there that needs to be done

— Alan Turing, Computing machinery and intelligence

The state of the art FE-based modelling of cable-pulley systems has been documented, and based on the obtained knowledge through the research, a full derivation of a two dimensional cable-pulley system has been proposed. However, the model has to be experimentally tested in order to fully verify it.

- The proposed model should be investigated by the upcoming PhD candidate, of whom is assigned to work further on this topic at the SFI project, and should be implemented in a custom designed program.

- A physical test rig of a system consisting of cable of pulleys, capable of provoking instabilities of the system should be built at the lab.

- Furthermore, it should be verified against physical tests experimentally, in order to accurately portray and render the dynamic behaviour, subsequently implementing sensor data rather than fictive loads. Thus, the model could be applied in control systems for stabilising the provoked out of phase tensions occurring.

- The work by Dr. Myhre [23] presented, states the in-house experience at NTNU with the ANCF-element, and demonstrates it capability of real-time simulations. A full derivation of the ANCF element formulated in Python is to be found at GitHub, developed by Dr. Myhre for his experiments described in Chapter 6, and is ready for deploying this purpose. Thus, Dr. Myhre could potentially function as a resource in on field of study. The work Dr. Myhre performed is very relevant when the cable-pulley model comes of maturity for combination with sensors, maybe vision based tracking on swinging heaves.

Bibliography

[1] Harold Kerzner. *Project Management : A Systems Approach to Planning, Scheduling, and Controlling*. Wiley, 2013.

[2] Salvatore T March and Gerald F Smith. Design and natural science research on information technology. *Decision Support Systems*, 15:251–266, 1995.

[3] Kathleen M Eisenhardt. Building Theories From Case Study Research. 1989.

[4] Alexander Kossiakoff. *Systems engineering : principles and practice*. Wiley-Interscience, 2011.

[5] Miguel Luiz Bucalem and Klaus-Jrgen Bathe. *The Mechanics of Solids and Structures - Hierarchical Modeling and the Finite Element Solution*. Computational Fluid and Solid Mechanics. Springer Berlin Heidelberg, Berlin, Heidelberg, 2011.

[6] Margaret. Cargill and Patrick O'Connor. *Writing scientific research articles : strategy and steps*. Wiley-Blackwell, Adelaide, Australia, second edition. edition, 2013.

[7] Fedem Technology. Fedem Release 7.2 Theory Guide. *Fedem Technology AS*, 2016.

[8] Ole Ivar Sivertsen. *Virtual testing of mechanical systems : theories and techniques*. Swets & Zeitlinger Publishers, 2001.

[9] Ivar Birkeland, Thuong Kim Than, Oddvar Birkeland, and Terje Rølvåg. Simulation of Dynamic Behaviour of a FPSO Crane. In *The 5th North Sea Offshore Crane Conference*, Aberdeen, Scotland, 2000.

[10] A Rouvinen, T Lehtinen, and P Korkealaakso. Container Gantry Crane Simulator for Operator Training. *Proceedings of the Institution of Mechanical Engineers, Part K: Journal of Multi-body Dynamics*, 219(4):325–336, 6 2005.

[11] A. Arena, A. Casalotti, W. Lacarbonara, and M.P. Cartmell. Dynamics of container cranes: three-dimensional modeling, full-scale experiments, and identification. *International Journal of Mechanical Sciences*, 93:8–21, 2015.

[12] U Lugrís, J L Escalona, D Dopico, and J Cuadrado. Efficient and accurate simulation of the rope-sheave interaction in weight-lifting machines. *Proceedings of the Institution of Mechanical Engineers, Part K: Journal of Multi-body Dynamics*, 225(4):331–343, 2011.

[13] F Ju and Y S Choo. Super element approach to cable passing through multiple pulleys. *International Journal of Solids and Structures 42*, 2004.

[14] Feng Ju and Yoo Sang Choo. Dynamic Analysis of Tower Cranes. *Journal of Engineering Mechanics*, 131(1), 2005.

[15] Kimmo S Kerkkänen, Daniel García-Vallejo, and Aki M Mikkola. Modeling of Belt-Drives Using a Large Deformation Finite Element Formulation. *Nonlinear Dynamics*, 43(3):239–256, 2006.

[16] K E Dufva, J T Sopanen, and A M Mikkola. A two-dimensional shear deformable beam element based on the absolute nodal coordinate formulation. *Journal of Sound and Vibration*, 280:719–738, 2005.

[17] Etsujiro Imanishi, Takao Nanjo, and Takahiro Kobayashi. Dynamic simulation of wire rope with contact. *Journal of Mechanical Science and Technology*, 23(4):1083–1088, 2009.

[18] F J Sun, Z H Zhu, and M Larosa. Dynamic modeling of cable towed body using nodal position finite element method. *Elsevier, Ocean Enginnering*, 2011.

[19] A A Shabana. Definition of the Slopes and the Finite Element Absolute Nodal Coordinate Formulation. *Multibody System Dynamics*, 1:339–348, 1997.

[20] Qingtao Wang, Qiang Tian, and Haiyan Hu. Dynamic simulation of frictional contacts of thin beams during large overall motions via absolute nodal coordinate formulation. *Nonlinear Dynamics*, 77(4):1411–1425, 2014.

[21] Qing-Tao Wang, Qiang Tian, and Hai-Yan Hu. Contact dynamics of elasto-plastic thin beams simulated via absolute nodal coordinate formulation. *Acta Mechanica Sinica*, 32(3):525–534, 6 2016.

[22] Qingtao Wang, Qiang Tian, and Haiyan Hu. Dynamic simulation of frictional multizone contacts of thin beams. *Nonlinear Dynamics*, 83(4):1919–1937, 2016.

[23] Torstein Anderssen Myhre. *Vision-based control of a robot interacting with moving and flexible objects*. PhD thesis, Norwegian University of Science and Technology, Trondheim, 2016.

[24] Radek Bulín, Michal Hajžman, and Pavel Polach. Nonlinear dynamics of a cablepulley system using the absolute nodal coordinate formulation. *Mechanics Research Communications*, 2016.

[25] Phil Andrew and Stefan Kaczmarczyk. Rope Dynamics Focus on Wire Ropes. *Elevator World, Inc*, 2011.

[26] Johannes Gerstmayr and Ahmed A Shabana. Analysis of Thin Beams and Cables Using the Absolute Nodal Co-ordinate Formulation. *Nonlinear Dynamics*, 45:109–130, 2006.

[27] Kaitlin S Spak, Gregory S Agnes, and Daniel J Inman. Modeling vibration response and damping of cables and cabled structures. *Journal of Sound and Vibration*, 336:240–256, 2014.

[28] Wire rope Aricraft Jacking, Aviation Structural Mechanic 3&2 - How airplanes are built and how to maintain them.

[29] K. O. Papailiou. On the bending stiffness of transmission line conductors. *IEEE Transactions on Power Delivery*, 12(4):1576–1583, 1997.

[30] Francesco Foti and Luca Martinelli. Mechanical modeling of metallic strands subjected to tension, torsion and bending. *International Journal of Solids and Structures*, 91:1–17, 2016.

[31] Fridtjov Irgens. *Formelsamling mekanikk*. Tapir Uttrykk, Trondheim, 3rd edition, 1999.

[32] Frederick G. F. Moritz. *Electromechanical motion systems : design and simulation*. Wiley, 2013.

[33] Yuxing Peng, Zhencai Zhu, Guoan Chen, and Jiusheng Bao. Numerical Analysis of Friction Lining's Temperature Field during Helically Sliding Contact with Wire Rope. In *2009 International Joint Conference on Computational Sciences and Optimization*, pages 237–241. IEEE, 4 2009.

[34] Yu-Xing Peng, Zhen-Cai Zhu, Min-Ming Tong, Guo-An Chen, Yan-Hai Cheng, Tong-Qing Li, Yi-Lei Li, Wan Ma, Chong-Qiu Wang, and Bin-Bin Liu. Thermostress coupling field of friction lining during high-speed slide of wire rope in a mine friction-drive hoist. *Journal of Mechanical Science*, 226 (9):2154 – 2167, 2011.

[35] W Ma and A A Lubrecht. Detailed contact pressure between wire rope and friction lining. *Tribology International 109 (2017) 238245 Contents*, 2017.

[36] J.L. Swayze and A. Akay. Effects of System Dynamics on Friction-Induced Oscillations. *Journal of Sound and Vibration*, 173(5):599–609, 6 1994.

[37] P Gdaniec, C Weiß, and N P Hoffmann. On chaotic friction induced vibration due to rate dependent friction. 2009.

[38] R Ibrahim. Friction Induced Vibrations. *Encyclopedia of Vibration - Knovel*, 1-3, 2001.

[39] M Aufaure. A finite element of cable passing through a pulley. *Computers & Structures*, 46(5):807–812, 1993.

[40] Dassault Systèmes S.A. Abaqus Analysis User's Guide, 2017.

[41] Daniel Priour. The Bar Finite Element for Cable 5.2 Tension on Bars. *A Finite Element Method for Netting, Application to Fish Cages and Fishing*, 2013.

[42] Ahmed A Shabana. Flexible Multibody Dynamics: Review of Past and Recent Developments. *Multibody System Dynamics*, 1(2):189–222, 1997.

[43] H. ASHLEY. Observations on the dynamic behavior of large flexible bodies in orbit. *AIAA Journal*, 5(3):460–469, 3 1967.

[44] J.R. Canavin and P.W. Likins. Floating Reference Frames for Flexible Spacecraft. *Journal of Spacecraft and Rockets*, 14(12):724–732, 12 1977.

[45] B Fraeijs and De Veubeke. The Dynamics of Flexible Bodies. *J. Engng*, 52(14):895–913, 1976.

[46] Ahmed A. Shabana and Refaat Y. Yakoub. Three Dimensional Absolute Nodal Coordinate Formulation for Beam Elements: Theory. *Journal of Mechanical Design*, 123(4):606, 2001.

[47] J L Escalona, H A Hussien, and A A Shabana. Application of the absolute nodal coordinate formulation to multibody system dynamics. *Journal of Sound and Vibration*, 214(sv981563):833–851, 1998.

[48] J B Jonker and J P Meijaard. A geometrically non-linear formulation of a three-dimensional beam element for solving large deflection multibody system problems. *International Journal of Non-Linear Mechanics*, 53:63–74, 2013.

[49] Kolbein Bell. *Engineering approach to finite element analysis of linear structural mechanics problems*. Fagbokforlaget, 2013.

[50] Stefan Von Dombrowski. Analysis of Large Flexible Body Deformation in Multibody Systems Using Absolute Coordinates. *Multibody System Dynamics*, 8:409–432, 2002.

[51] Daniel García-Vallejo, Aki M Mikkola, and Jos Luis Escalona. A new locking-free shear deformable finite element based on absolute nodal coordinates. *Nonlinear Dynamics*, 50(1):249–264, 2007.

[52] Karin Nachbagauer, Astrid S Pechstein, Hans Irschik, Johannes Gerstmayr, K Nachbagauer, A S Pechstein, H Irschik, H Irschik, and J Gerstmayr. A new locking-free formulation for planar, shear deformable, linear and quadratic beam finite elements based on the absolute nodal coordinate formulation. *Multibody Syst Dyn*, 26:245–263, 2011.

[53] Naresh Khude, Ilinca Stanciulescu, Daniel Melanz, and Dan Negrut. Efficient Parallel Simulation of Large Flexible Body Systems With Multiple Contacts. *Journal of Computational and Nonlinear Dynamics*, 8(4):041003, 3 2013.

[54] Ahmed A. Shabana. Floating Frame of Reference Formulation. In Ahmed A Shabana, editor, *Dynamics of Multibody Systems*, pages 185–262. Cambridge University Press, Cambridge, 4 edition, 2013.

[55] Peter Betsch and SpringerLink. *Structure-preserving Integrators in Nonlinear Structural Dynamics and Flexible Multibody Dynamics*, volume 565. Springer International Publishing : Imprint: Springer, 2016.

[56] D García-Vallejo, J L Escalona, J Mayo, and J Domínguez. Describing Rigid-Flexible Multibody Systems Using Absolute Coordinates. *Nonlinear Dynamics*, 34:75–94, 2003.

[57] Kaitlin Spak, Gregory Agnes, and Daniel Inman. Cable Parameters for Homogenous Cable-Beam Models for Space Structures. pages 7–18. Springer, Cham, 2014.

[58] Ahmed A. Shabana. The Large Deformation Problem. In Ahmed A Shabana, editor, *Dynamics of Multibody Systems*, pages 304–338. Cambridge University Press, Cambridge, 4 edition, 2013.

[59] J Garcia De Jalgn, J Unda, and A Avello. Natural coordinates for the computer analysis of multibody systems. *Elsevier Science Publishers B.V (North-Holland)*, 1986.

[60] Javier García de Jalón and Eduardo Bayo. *Kinematic and Dynamic Simulation of Multibody Systems*. Mechanical Engineering Series. Springer New York, New York, NY, 1994.

[61] Margarida Machado, Pedro Moreira, Paulo Flores, and Hamid M Lankarani. Compliant contact force models in multibody dynamics: Evolution of the Hertz contact theory. *MAMT*, 53:99–121, 2012.

[62] P Flores, J Ambrósio, J C P Claro, and H M Lankarani. Influence of the contactimpact force model on the dynamic response of multi-body systems. *Proceedings of the Institution of Mechanical Engineers, Part K: Journal of Multi-body Dynamics*, 220(1):21–34, 1 2006.

[63] H M Lankarani and P E Nikravesh. A Contact Force Model With Hysteresis Damping for Impact Analysis of Multibody Systems. *Journal of Mechanical Design*, 112, 1990.

[64] Kenneth Hunt and Erskine Crossley. Coefficient of restitution interpreted as damping in vibroimpact. *Journal of Applied Mechanics, American Society of Mechanical Engineers*, 1975.

[65] Yves Gonthier, John Mcphee, Christian Lange, and Jean-Claude Piedboeuf. A Regularized Contact Model with Asymmetric Damping and Dwell-Time Dependent Friction. *Multibody System Dynamics*, 11:209–233, 2004.

[66] Jung Ching Chung. Elasticplastic contact analysis of an ellipsoid and a rigid flat. *Tribiology International*, 43:491–502, 2009.

[67] C Pereira, A Ramalho, J Ambrosio, B J Ambrosio, Jorge Ambrosio@tecnico Ulisboa Pt, Candida@isec Pt, and A Ramalho. An enhanced cylindrical contact force model. *Multibody Syst Dyn*, 35:277–298, 2015.

[68] Johannes. Brandlein. *Die Walzlagerpraxis : Handbuch fur die Berechnung und Gestaltung von Lagerungen*. Vereinigte Fachverl, 3rd edition, 1998.

[69] Ho-Young Cha, Juhwan Choi, Han Sik Ryu, and Jin Hwan Choi. Stick-slip algorithm in a tangential contact force model for multi-body system dynamics. *Journal of Mechanical Science and Technology*, 25(7):1687, 2011.

[70] Brian Armstrong-Hélouvry. *Control of Machines with Friction*. Springer US, Boston, MA, 1991.

[71] C. Canudas de Wit, H. Olsson, K.J. Astrom, and P. Lischinsky. A new model for control of systems with friction. *IEEE Transactions on Automatic Control*, 40(3):419–425, 3 1995.

[72] Ahmed A. Shabana. Analytical Techniques. In Ahmed A Shabana, editor, *Dynamics of Multibody Systems*, pages 83–156. Cambridge University Press, Cambridge, 4 edition, 2013.

[73] M Hajžman and P Polach. Application of stabilization techniques in the dynamic analysis of multibody systems. *Applied and Computational Mechanics 1 (2007)*, 2007.

[74] J Oliver, S Hartmann, J C Cante, R Weyler, and J A Hernández. A contact domain method for large deformation frictional contact problems. Part 1: Theoretical basis. *Comput. Methods Appl. Mech. Engrg*, 198:2591–2606, 2009.

[75] Peter Wriggers and Tod A Laursen. *Computational Contact Mechanics*. Springer-WienNewYork, 2007.

[76] Carlos A. Felippa. Introduction to Finite Element Methods, 2004.

[77] Magnus R. Hestenes. Multiplier and gradient methods. *Journal of Optimization Theory and Applications*, 4(5):303–320, 11 1969.

[78] J Cuadrado, R Gutiérrez, M A Naya, and M González. Experimental Validation of a Flexible MBS Dynamic Formulation through Comparison between Measured and Calculated Stresses on a Prototype Car. *Multibody System Dynamics*, 11(2):147–166, 2004.

[79] N. M. Newmark. A method of computation for structural dynamics. Journal of Engineering Mechanics. *ASCE*, 85 (EM3):67–94, 1959.

[80] ShuennYih Chang. Investigation of WBZ [alpha] method for solving nonlinear systems. *Engineering Computations*, 24(4):384–406, 6 2007.

[81] Hans M. Hilber, Thomas J. R. Hughes, and Robert L. Taylor. Improved numerical dissipation for time integration algorithms in structural dynamics. *Earthquake Engineering & Structural Dynamics*, 5(3):283–292, 7 1977.

[82] Kevin Burrage. Efficiently Implementable Algebraically Stable Runge-Kutta Methods. *SIAM Journal on Numerical Analysis*, 19(2):245–258, 1982.

[83] Edward J. Haug and Roderic C. Deyo, editors. *Real-Time Integration Methods for Mechanical System Simulation*. Springer Berlin Heidelberg, Berlin, Heidelberg, 1991.

[84] G. N. Pande and S. Pietruszczak. *Numerical models in geomechanics : NUMOG IX*. A.A. Balkema, 2004.

[85] J Chung and G M Hulbert. A Time Integration Algorithm for Structural Dynamics With Improved Numerical Dissipation: The Generalized-α Method. *Journal of Applied Mechanics*, 60(2):371–375, 6 1993.

[86] Naresh N Khude. *Efficient simulation of flexible body systems with frictional contact/impact*. PhD thesis, University of Wisconsin-Madison, 2015.

[87] Alexander Konyukhov and Karl Schweizerhof. *Computational Contact Mechanics*. Springer-Verlag Berlin Heidelberg 2013, 2013.

[88] W Schiehlen. Multibody System Dynamics: Roots and Perspectives. *Multibody System Dynamics*, 1:149–188, 1997.

A

Risk Assessment

Enhet: IMP

Dato: 30.01.17

Linjeleder: Torgeir Welo

Deltakere ved kartleggingen (m/ funksjon): Jon Andreas Moseid (Student) Professor Terje Rølvåg (Veileder)
(Ansv. veileder, student, evt. medveiledere, evt. andre m. kompetanse)

Kort beskrivelse av hovedaktivitet/hovedprosess: Masteroppgave for Jon Andreas Moseid. Crane modeling and production for cable and pulley development

Er oppgaven rent teoretisk? (JA/NEI): NEI   *«JA» betyr at veileder innestår for at oppgaven ikke inneholder noen aktiviteter som krever risikovurdering. Dersom «JA»: Beskriv kort aktiviteten i kartleggingskjemaet under. Risikovurdering trenger ikke å fylles ut.*

Signaturer: *Ansvarlig veileder:*   *Student:*

ID nr.	Aktivitet/prosess	Ansvarlig	Eksisterende dokumentasjon	Eksisterende sikringstiltak	Lov, forskrift o.l.	Kommentar
01	Litteraturstudie	Jon Andreas Moseid	Prosjektbeskrivelse	-	-	Kontorarbeid
02	Software arbeid i FEDEM (Virtuell tvilling)	Jon Andreas Moseid	Prosjektbeskrivelse	-	-	Kontorarbeid
03	Lab arbeid med Fysisk tvilling, instrumentering av sensorer.	Jon Andreas Moseid	Prosjektbeskrivelse	SJA	-	Verksted/Lab
04	Programmering	Jon Andreas Moseid	Prosjektbeskrivelse	-	-	Kontorarbeid

Enhet: **Dato:**

Linjeleder:

Deltakere ved kartleggingen (m/ funksjon):
(Ansv. Veileder, student, evt. medveiledere, evt. andre m. kompetanse)

Risikovurderingen gjelder hovedaktivitet: Masteroppgave student xx. Tittel på oppgaven.

Signaturer: *Ansvarlig veileder:*   *Student:*

ID nr	Aktivitet fra kartleggings- skjemaet	Mulig uønsket hendelse/ belastning	Vurdering av sannsyn- lighet (1-5)	Vurdering av konsekvens:				Risiko- Verdi (menn- eske)	Kommentarer/ status Forslag til tiltak
				Menneske (A-E)	Ytre miljø (A-E)	Øk/ materiell (A-E)	Om- dømme (A-E)		
01	Litteraturstudie	Vond nakke, vond rygg, sår setemuskulatur, senebetennelse	3	B	A	A	A	B3	Øke fysisk aktivitetsnivå i løpet av arbeidsdagen
02	Software arbeid i FEDEM (Virtuell tvilling)	Vond nakke, vond rygg, sår setemuskulatur, senebetennelse	3	B	A	A	A	B3	Øke fysisk aktivitetsnivå i løpet av arbeidsdagen
03	Lab arbeid med instrumentering av fysisk tvilling	Strømstøt, kjemisk kontakt, kutt, klemskade.	2	C	A	B	A	C2	Utføre SJA før LAB
04	Programmering	Vond nakke, vond rygg, sår setemuskulatur, senebetennelse	3	B	A	A	A	B3	Øke fysisk aktivitetsnivå i løpet av arbeidsdagen

Sannsynlighet vurderes etter følgende kriterier:

Svært liten 1	Liten 2	Middels 3	Stor 4	Svært stor 5
1 gang pr 50 år eller sjeldnere	1 gang pr 10 år eller sjeldnere	1 gang pr år eller sjeldnere	1 gang pr måned eller sjeldnere	Skjer ukentlig

Konsekvens vurderes etter følgende kriterier:

Gradering	Menneske	Ytre miljø Vann, jord og luft	Øk/materiell	Omdømme
E Svært Alvorlig	Død	Svært langvarig og ikke reversibel skade	Drifts- eller aktivitetsstans >1 år.	Troverdighet og respekt betydelig og varig svekket
D Alvorlig	Alvorlig personskade. Mulig uførhet.	Langvarig skade. Lang restitusjonstid	Driftsstans > ½ år Aktivitetsstans i opp til 1 år	Troverdighet og respekt betydelig svekket
C Moderat	Alvorlig personskade.	Mindre skade og lang restitusjonstid	Drifts- eller aktivitetsstans < 1 mnd	Troverdighet og respekt svekket
B Liten	Skade som krever medisinsk behandling	Mindre skade og kort restitusjonstid	Drifts- eller aktivitetsstans < 1uke	Negativ påvirkning på troverdighet og respekt
A Svært liten	Skade som krever førstehjelp	Ubetydelig skade og kort restitusjonstid	Drifts- eller aktivitetsstans < 1dag	Liten påvirkning på troverdighet og respekt

Risikoverdi = Sannsynlighet x Konsekvens
Beregn risikoverdi for Menneske. Enheten vurderer selv om de i tillegg vil beregne risikoverdi for Ytre miljø, Økonomi/materiell og Omdømme. I så fall beregnes disse hver for seg.

Til kolonnen "Kommentarer/status, forslag til forebyggende og korrigerende tiltak":
Tiltak kan påvirke både sannsynlighet og konsekvens. Prioriter tiltak som kan forhindre at hendelsen inntreffer, dvs. sannsynlighetsreduserende tiltak foran skjerpet beredskap, dvs. konsekvensreduserende tiltak.

NTNU		utarbeidet av	Nummer	Dato
	Risikomatrise	HMS-avd.	HMSRV2604	08.03.2010
		godkjent av	Erstatter	
HMS/KS		Rektor		09.02.2010

MATRISE FOR RISIKOVURDERINGER ved NTNU

	Svært liten	Liten	Middels	Stor	Svært stor
Svært alvorlig	E1	E2	E3	E4	E5
Alvorlig	D1	D2	D3	D4	D5
Moderat	C1	C2	C3	C4	C5
Liten	B1	B2	B3	B4	B5
Svært liten	A1	A2	A3	A4	A5
	Svært liten	Liten	Middels	Stor	Svært stor
			SANNSYNLIGHET		

Prinsipp over akseptkriterium. Forklaring av fargene som er brukt i risikomatrisen.

Farge		Beskrivelse
Rød		Uakseptabel risiko. Tiltak skal gjennomføres for å redusere risikoen.
Gul		Vurderingsområde. Tiltak skal vurderes.
Grønn		Akseptabel risiko. Tiltak kan vurderes ut fra andre hensyn.

Appendix B

Spatial contact kinematics between cable and pulley

In order to define constraints to a multibody system containing components subjected to large displacements and deflections, an algorithm for determining contact between the objects is vital. A natural measure of contact interaction has become the CPP procedure, also known as the minimal distance criterion, which most important operation for data transfer between contacting bodies [20, 87]. In this case, one seeks the projection between an arbitrary contact point on a curve, and a surface representing the pulley. It is well known within FEM theory, an object dominating the contact conditions is considered the so called "master" element, where the dependent object is known as a "slave" element. Since the pulley can be considered as rigid in comparison with a cable, the surface becomes the master object. The discussed contact formulation in this section, is manly inspired by the works performed by Bulín et al. [24], and the works performed in an ongoing research by Wang et al.[20, 22, 21] who applies a so called Closest Point Projection (CPP) procedure in order to detect contact before applying the master-slave technique for defining constraint conditions. The contact formulation is mainly based on theory provided by the literature of Konyukhov and Schweizerhof[87].

In figure B.1, the kinematics of a curve to a rigid surface is illustrated, the curve is defined in a Serret-Frenet coordinate system, and the surface in a Gaussian system. A surface representing the boundary of a three dimensional solid can be parameterized by local co-ordinates ξ_1 and ξ_2. The vector $\boldsymbol{\rho}(\xi_1, \xi_2)$ describes an arbitrary point on the surface [87], and is expressed

$$\boldsymbol{\rho}(\xi_1, \xi_2) = \sum_k N_k(\xi_1, \xi_2)\mathbf{x}^k \ k = 1, 2, 3, ..., n \tag{B.1}$$

$N_k(\xi_1, \xi_2)$ and $\mathbf{x}^k$ represents the shape functions (if any) of the surface and the nodal coordinates respectively. A spatial coordinate system describing the geometrical properties of the surface is introduced, constructed by surface tangents and normal vector which yields
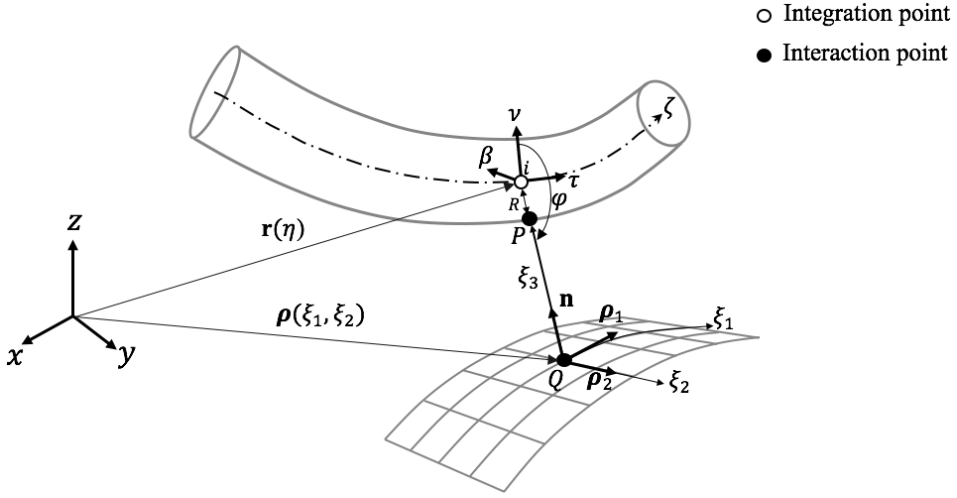
Figure B.1: Curve to surface

$$\boldsymbol{\rho}_1 = \frac{\partial \boldsymbol{\rho}}{\partial \xi_1}, \quad \boldsymbol{\rho}_2 = \frac{\partial \boldsymbol{\rho}}{\partial \xi_2}, \quad \mathbf{n} = \frac{\boldsymbol{\rho}_1 \times \boldsymbol{\rho}_2}{\left| \boldsymbol{\rho}_1 \times \boldsymbol{\rho}_2 \right|} \tag{B.2}$$

The CPP projection allows to define a new coordinate system related to the surface coordinate system as follows

$$\mathbf{r}(\xi_1, \xi_2, \xi_3) = \boldsymbol{\rho}(\xi_1, \xi_2) + \mathbf{n}\xi_3 \tag{B.3}$$

where vector $\mathbf{r}(\xi_1, \xi_1, \xi_1)$ describes the "slave" point. Considering a beam formulated by ANCF is illustrated in figure B.1, a new Serret-Frenet (Appendix C) coordinate system τ, ν, β, known from differential geometry, are introduced to be defined at any point of the curve [87]. The axial local body coordinate system of the assembled cable ζ [20], is defined as

$$\zeta = \bar{\zeta} + \hat{\zeta} \tag{B.4}$$

where $\bar{\zeta} \in [0 \quad 1]$ is denoting the decimal part of ζ, and $\hat{\zeta} \in [0 \quad n]$ where n represents the number of elements used for meshing the beams. It is also worth noting $\bar{\zeta}$ from equals ξ from equation 7.3 according to its definition. Introducing contact points on the curve η_i where $\mathbf{r}(\eta)$ denotes its position in the global coordinate system.

$$\mathbf{r}(\eta) = \boldsymbol{\rho}(\xi_1, \xi_2) + \mathbf{n}\xi_3 \tag{B.5}$$

Introducing the measure of a contact point on the surface of a cable with respect to its radius yields

$$\xi_3 = (\mathbf{r}(\eta) - \boldsymbol{\rho}(\xi_1, \xi_2))\mathbf{n} - R \tag{B.6}$$

where the shortest distance ξ_3 is considered penetration. In order to determine contact conditions, the CPP is applied, normally solved by Newtons method.

$$\begin{cases} \xi_3 > 0 \Rightarrow \text{no contact} \\ \xi_3 \leqslant 0 \Rightarrow \text{contact} \end{cases}$$

Contact is obtained when a slave point penetrates into the master surface, however, for exact representations such as Lagrangian contact. When contact is detected, the kinematic relations of the contacting bodies in the considered point as means for applying the principle of virtual work for establishing the forces occurring during contact.

The relative kinematics of cable-pulley

During interaction, the slave point shares the coordinates of the master surface and its local coordinates, ξ_1, ξ_2, ξ_3, with the assumption of a moving surface makes $\boldsymbol{\rho}(t, \xi_1, \xi_2, \xi_3)$ and $\mathbf{n}(t, \xi_1, \xi_2, \xi_3)$ time dependent. The translational velocity of point Q on the surface has the velocity

$$\mathbf{v}_Q = \frac{\partial \boldsymbol{\rho}}{\partial t} \tag{B.7}$$

The velocity of point P relative to Q is expressed by the time derivative describing its motion

$$\mathbf{v}_P = \frac{d}{dt} \mathbf{r}_P(t, \xi_1, \xi_2, \xi_3) = \frac{d}{dt} \boldsymbol{\rho} + \frac{d}{dt}(\mathbf{n}\xi_3)$$

$$= \frac{\partial \boldsymbol{\rho}}{\partial t} + \frac{\partial \boldsymbol{\rho}}{\partial \xi_j} \dot{\xi}_j + \frac{\partial \mathbf{n}}{\partial t} \xi_3 + \mathbf{n}\dot{\xi}_3 + \frac{\partial \mathbf{n}}{\partial \xi_j} \xi_3 \dot{\xi}_j, \qquad j = 1, 2. \tag{B.8}$$

equation B.8 can be rewritten according to the Weingarten formula to the following form

$$\mathbf{v}_P = \mathbf{v}_Q + \xi_3 \frac{\partial \mathbf{n}}{\partial t} + \mathbf{n}\dot{\xi}_3 + (\boldsymbol{\rho} - \xi_3 h_j^i \boldsymbol{\rho}_i), \qquad i, j = 1, 2. \tag{B.9}$$

The difference of these two velocities yields a relative velocity, $\mathbf{v}_r$, between the contacting bodies. Considering the relative velocities between the contacting bodies, starting with the cables tangential motion relative to the surface

$$\mathbf{v}_P - \mathbf{v}_Q = \dot{\xi}_3 \mathbf{n} + \dot{\xi}_j \boldsymbol{\rho}_i, \qquad i, j = 1, 2. \tag{B.10}$$

and the surface motion relative to the cable. Opposite, operating from the from a fixed point on the cable in the Serret-Frenet C system, the motion of the pulley relative to the cable is expressed

$$\mathbf{v}_Q - \mathbf{v}_P = \nu_\tau \boldsymbol{\tau} + \nu_e \mathbf{e} + \nu_g \mathbf{g} \tag{B.11}$$

$$\mathbf{e} = \frac{\boldsymbol{\rho} - \mathbf{r}_P}{||\boldsymbol{\rho} - \mathbf{r}_P||} = -\mathbf{n} \tag{B.12}$$

By summarizing equation B.10 and B.11 the following expression is obtained

$$\dot{\xi}_3 \mathbf{n} + \dot{\xi}_j \boldsymbol{\rho}_i + \nu_\tau \boldsymbol{\tau} + \nu_e \mathbf{e} + \nu_g \mathbf{g} = 0 \tag{B.13}$$

The variation of the relative normal displacement

$$\delta u_e = \delta \xi_3 = (\delta \boldsymbol{\rho} - \delta \mathbf{r}_P) \cdot \mathbf{e} \tag{B.14}$$

The pulling velocity, i.e. relative to the axis of the cable

$$\delta u_\tau = -(\boldsymbol{\rho}_i \cdot \tau) \dot{\xi}_j \tag{B.15}$$

The dragging velocity, i.e. relative to the axis of the cable

$$\delta u_{\mathbf{g}} = -(\boldsymbol{\rho}_i \cdot \mathbf{g}) \dot{\xi}_j \tag{B.16}$$

Now all the expressions for the relative displacements between the cable and pulley is derived, summarizing them into one equation we obtain its expression in weak form

$$\delta \boldsymbol{\rho} - \delta \mathbf{r}_P = \delta u_\tau \boldsymbol{\tau} + \delta u_{\mathbf{e}} \mathbf{e} + \delta u_{\mathbf{g}} \mathbf{g} \tag{B.17}$$

Integrating it we obtain the motion for a time step in a weak form

$$\int (\delta \boldsymbol{\rho} - \delta \mathbf{r}_P) \tag{B.18}$$

in which one obtain contact forces from, in all three directions of the cable moving along a surface.
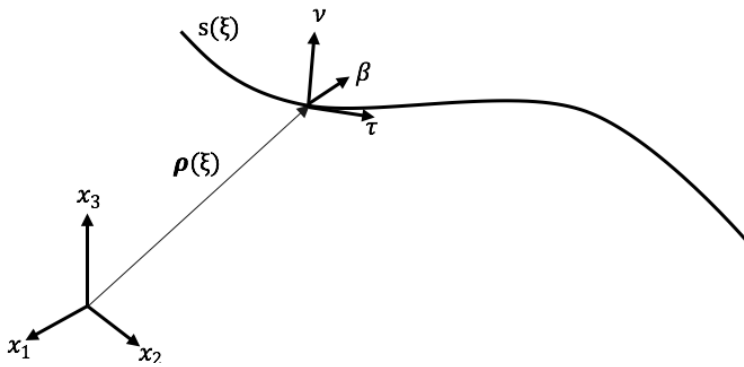
Appendix C

Serret-Frenet coordinate system

Figure C.1: Serret-Frenet coordinate system on a spatial curve

Considering an arbitrary curve in a tree dimensional Cartesian coordinate system, described by a parameter ξ. Assuming a continuously differentiable (C^1) expression with respect to ξ, the vector can be written in parametrc from

$$\boldsymbol{\rho} = \boldsymbol{\rho}(\xi) = \begin{bmatrix} x_1(\xi) \\ x_2(\xi) \\ x_3(\xi) \end{bmatrix} \tag{C.1}$$

A differential of the arc-length s of the curve in the natural coordinate system is

$$ds = ds(\xi) = \sqrt{\boldsymbol{\rho}_\xi \cdot \boldsymbol{\rho}_\xi} d\xi = \mathbf{J} d\xi \tag{C.2}$$

where $\mathbf{J}$ is the Jacobian of the transformation between s and ξ. A Serret-Frenet corrdinate system is defined by three unit-vectors which is attached along a smooth continuous curve. A unit tangent vector τ, a unit normal vector ν pointing to the curvature centre, and the cross product β forming a bi-normal vector.

$$\beta = \tau \times \nu \tag{C.3}$$

These unit vectors relates to the global coordinate system via the derivative of the curve ρ with respect to the arc lenght s, and are commonly referred to in differential geometry as the Serret-Frenet formulas:

$$\begin{cases} \frac{d\tau}{ds} = \kappa\nu \\ \frac{d\nu}{ds} = -\kappa\tau + \chi\beta \\ \frac{d\beta}{ds} = -\chi\nu \end{cases} \tag{C.4}$$

Where κ denotes a curvature and χ the torsion of a spatial curve, the curvature and the torsion can be computed as follows

$$\kappa\beta = \frac{\rho_\xi \times \rho_{\xi\xi}}{\left|\rho_\xi\right|^3} \rightarrow \kappa = \frac{\rho_\xi \times \rho_{\xi\xi}}{\left|\rho_\xi\right|^3} \tag{C.5}$$

$$\chi = \frac{det(\rho_\xi, \rho_{\xi\xi}, \frac{\partial^3 \rho}{\partial \xi^3})}{\left|\rho_\xi \times \rho_{\xi\xi}\right|} = \frac{(\rho_\xi \times \rho_{\xi\xi}) \cdot \frac{\partial^3 \rho}{\partial \xi^3}}{\left|\rho_\xi \times \rho_{\xi\xi}\right|} \tag{C.6}$$

Classic equations for cable and pulleys

Some general equations mathematical formulations of cable and pulleys can is illustrated in this section. The formulations is to be found in Irgens [31]
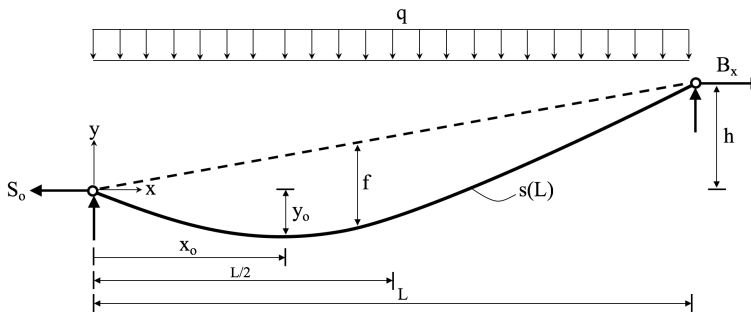
Cable

Figure D.1: Asymmetric planar cable

Shape:

$$y(x) = \frac{q}{2S_0}(x^2 - Lx) + \frac{hx}{L} \tag{D.1}$$

$$S_0 = \frac{qL^2}{8f} \tag{D.2}$$

$$f = \frac{qL^2}{8S_0} = \frac{h}{4} - \frac{y_0}{2} + \frac{1}{2}\sqrt{y_0^2 - y_0 h} \tag{D.3}$$

Axial tension:

$$S = \sqrt{S_0^2 + \left[q\frac{x-L}{2} + S_0\frac{h}{l} \right]^2} \tag{D.4}$$

$$S_{max} = S_0\sqrt{1 + \left[\frac{ql}{2S_0} + \frac{h}{L} \right]^2} \tag{D.5}$$

Pulley

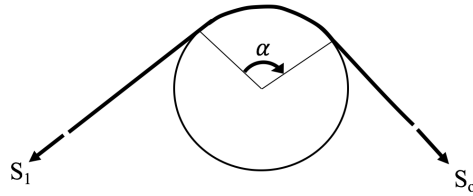**Figure D.2:** Simple pulley friction

$$S_1 = S_0 e^{-\mu\alpha} \tag{D.6}$$

Ellipsoidal to surface contact

$$K_{elip} = \frac{4}{3(\sigma_i + \sigma_j)}\sqrt{R_i}, \qquad \sigma_l = \frac{1-\nu_l^2}{E_l}, \qquad l = i, j \tag{D.7}$$

In cases of Parabolic distribution of contact stresses, $n = 1.5$